



This is a repository copy of *Developmental and biophysical determinants of grass leaf size worldwide*.

White Rose Research Online URL for this paper:  
<https://eprints.whiterose.ac.uk/175462/>

Version: Accepted Version

---

**Article:**

Baird, A.S., Taylor, S.H., Pasquet-Kok, J. et al. (8 more authors) (2021) Developmental and biophysical determinants of grass leaf size worldwide. *Nature*, 592 (7853). pp. 242-247. ISSN 0028-0836

<https://doi.org/10.1038/s41586-021-03370-0>

---

This is a post-peer-review, pre-copyedit version of an article published in *Nature*. The final authenticated version is available online at: <http://dx.doi.org/10.1038/s41586-021-03370-0>.

**Reuse**

Items deposited in White Rose Research Online are protected by copyright, with all rights reserved unless indicated otherwise. They may be downloaded and/or printed for private study, or other acts as permitted by national copyright laws. The publisher or other rights holders may allow further reproduction and re-use of the full text version. This is indicated by the licence information on the White Rose Research Online record for the item.

**Takedown**

If you consider content in White Rose Research Online to be in breach of UK law, please notify us by emailing [eprints@whiterose.ac.uk](mailto:eprints@whiterose.ac.uk) including the URL of the record and the reason for the withdrawal request.



[eprints@whiterose.ac.uk](mailto:eprints@whiterose.ac.uk)  
<https://eprints.whiterose.ac.uk/>

1 **Developmental and biophysical determinants of grass leaf size worldwide**

2

3 **Authors:** *Alec S. Baird<sup>1\*</sup>, Samuel H. Taylor<sup>2,3</sup>, Jessica Pasquet-Kok<sup>1</sup>, Christine Vuong<sup>1</sup>, Yu*  
4 *Zhang<sup>1</sup>, Teera Watcharamongkol<sup>3,4</sup>, Christine Scoffoni<sup>1,5</sup>, Erika J. Edwards<sup>6</sup>, Pascal-Antoine*  
5 *Christin<sup>3</sup>, Colin P. Osborne<sup>3</sup>, Lawren Sack<sup>1\*</sup>*

6

7 **Affiliations:**

8 <sup>1</sup>Department of Ecology and Evolutionary Biology, University of California Los Angeles, 621  
9 Charles E. Young Drive South, Los Angeles, CA 90095, USA.

10 <sup>2</sup>Lancaster Environment Centre, University of Lancaster, Lancaster LA1 4YW, UK.

11 <sup>3</sup>Department of Animal and Plant Sciences, University of Sheffield, Sheffield S10 2TN, UK.

12 <sup>4</sup>Faculty of Science and Technology, Kanchanaburi Rajabhat University, Muang District,  
13 Kanchanaburi, Thailand 7100.

14 <sup>5</sup>Department of Biological Sciences, California State University Los Angeles, 5151 State  
15 University Drive, Los Angeles, CA 90032, USA.

16 <sup>6</sup>Department of Ecology and Evolutionary Biology, Yale University, New Haven, CT 06520,  
17 USA.

18 \*Correspondence to: [alecsbaird@gmail.com](mailto:alecsbaird@gmail.com) and [lawrensack@ucla.edu](mailto:lawrensack@ucla.edu)

19

20 **Abstract**

21

22 **One of the most striking ecological trends is the association of small leaves with dry and**  
23 **cold climates, described 2400 years ago by Theophrastus, and recently recognized for**  
24 **eudicotyledonous plants at the global scale<sup>1-3</sup>. For eudicotyledons, this pattern is attributed**  
25 **to small leaves having a thinner boundary layer to avoid extreme leaf temperatures<sup>4</sup>, and**  
26 **their developing vein traits that improve water transport under cold or dry climates<sup>5,6</sup>. Yet,**  
27 **the global distribution of leaf size and its mechanisms have not been tested in grasses, an**  
28 **extraordinarily diverse lineage, distinct in leaf morphology, which contributes 33% of**  
29 **terrestrial primary productivity, including the bulk of crop production<sup>7</sup>. Here we**  
30 **demonstrate that grasses have shorter and narrower leaves under colder and drier climates**  
31 **worldwide. We show that small grass leaves have thermal advantages and vein**  
32 **development that contrast with those of eudicotyledons, but that also explain the**  
33 **abundance of small leaves in cold and dry climates. The worldwide distribution of grass**  
34 **leaf size exemplifies how biophysical and developmental processes result in convergence**  
35 **across major lineages in adaptation to climate globally, and highlights the importance of**  
36 **leaf size and venation architecture for grass performance in past, present and future**  
37 **ecosystems.**

38 The grasses (family Poaceae) originated at least 55 Mya<sup>8</sup> and include ~11,500 species in 750  
39 genera<sup>9</sup>, dominating up to 43% of the Earth’s surface<sup>7</sup> (Fig. 1). Small leaves have been linked  
40 with arid climates in specific grass lineages and communities (Supplementary Table 1). A  
41 worldwide climatic association could importantly influence species’ distributions, tolerance of  
42 climate change, and crop breeding. We tested relationships of leaf size with climate across 1752  
43 grass species from 373 genera in a global database and for 27 diverse and globally distributed  
44 species in a common garden (Extended Data Fig. 1, Supplementary Table 2 and 3).

45 We also tested for an adaptive basis for the association of grass leaf size with climate  
46 (Fig. 1). Because smaller leaves couple more tightly with air temperature due to their thinner  
47 boundary layer, small-leafed eudicots avoid damage from night-time chilling and daytime  
48 overheating<sup>4</sup>, and they may also achieve higher photosynthetic rate and water use efficiency and  
49 compensate for shorter growing periods<sup>4,10-12</sup>. We evaluated these potential advantages for small  
50 leafed grasses using energy balance modeling.

51 Smaller leaves may also develop vein traits that confer stress tolerance<sup>5</sup>. In typical  
52 eudicots, the large (“major”) veins are patterned before the bulk of leaf expansion<sup>5</sup>, and leaves  
53 that expand less have narrower major veins and xylem conduits, and major veins more closely  
54 spaced, resulting in a higher major vein length per leaf area (major VLA)<sup>5,6</sup>. Across eudicots,  
55 major vein traits scale allometrically with mature leaf size:

$$56 \quad \text{Trait} = a \times \text{leaf area}^b \quad (1)$$

57 where  $a$  is a scaling coefficient and  $b$  the scaling exponent<sup>13</sup>. These major vein traits in small  
58 eudicot leaves can provide greater water transport and lower vulnerability to freezing and  
59 dehydration<sup>6</sup> (Fig. 1a, Supplementary Table 4). Yet grass leaves are highly distinct, with parallel  
60 longitudinal veins connected by transverse veins<sup>14</sup>. To determine vein scaling, and its adaptive  
61 consequences for small grass leaves, we synthesized a model of C<sub>3</sub> and C<sub>4</sub> grass leaf  
62 development (Box 1, Table 1). For 27 grass species in a common garden, we compared the  
63 predicted scaling relationships against null expectations from geometric scaling<sup>5,13</sup> (Extended  
64 Data Fig. 1, Supplementary Table 3). We tested whether developmental scaling would confer  
65 small leaves with potential climatic advantages.

**Box 1.** *Synthetic model of grass leaf vein development based on published data for 20 species (Supplementary Tables 5-6), conferring small leaves with traits advantageous under cold and dry climates*

Grass leaf development includes five phases based on developmental zones:

**Phase P (formation and expansion of the primordium, P):** “Founder cells” in the periphery of the shoot apical meristem generate the leaf primordium. Cell divisions drive growth of a hood-like structure, in which the central 1° vein (midvein) and the large 2° veins are initiated early and extend acropetally, enabling their prolonged diameter growth (Box 1 Fig. 1a, c, e). Henceforth, discrete spatial growth zones develop at the leaf base and drive leaf expansion laterally and longitudinally.

**Phase D (formation of the cell division zone, DZ):** The basal cell division zone (DZ) expands slightly, driving minimal growth (Box 1 Fig. 1a, b). The 1° and 2° vein orders (major veins) complete their patterning basipetally along the leaf blade and increase in diameter (Box 1 Fig. 1c, e). Meanwhile, beginning at the lamina tip, C<sub>3</sub> species form a single order of small longitudinal minor veins, i.e., 3° veins, as do most C<sub>4</sub> species, i.e., C<sub>4-3L</sub> species. Some C<sub>4</sub> species of the subfamily Panicoideae additionally form smaller 4° veins, i.e., C<sub>4-4L</sub> species<sup>15</sup> (Box 1 Fig. 1c).

**Phase D-E (DZ, and formation of the expansion zone, EZ):** Cells from the DZ transition to a distinct, distal expansion zone (EZ). In the EZ, cell expansion in width and length spaces apart the 1° and 2° veins, resulting in the declines in their vein length per leaf area (Box 1 Fig. 1a, b, d). Additional 3° veins (and in some species, 4° veins) continue to initiate at the leaf tip between major vein orders and extend basipetally (Box 1 Fig. 1c-e). The transverse 5° veins form last, connecting the longitudinal veins.

**Phase D-E-M (DZ, EZ and the maturation zone, MZ):** Cells from the EZ mature distally, generating the maturation zone (MZ), which increases in size as cells file through the developmental zones (Box 1 Fig. 1a). The venation xylem, phloem and bundle sheath mature.

**Phase M (all leaf is MZ):** Leaf development is complete with all cells differentiated and expanded (Box 1 Fig. 1a-b).

Given that this developmental model is conserved across grass species, scaling predictions can be derived for species varying in leaf size (Supplementary Table 6). Some of these scaling relationships arise intrinsically from the sequence of development. Thus, major vein length per area (VLA) would be lower in wider leaves, as their major veins are spaced further apart. The 1° VLA declines geometrically as the inverse of leaf width, whereas the 2° VLA would decline less steeply than geometrically, as the formation of more 2° veins would partially counteract their greater spacing. Other scaling trends are not intrinsic, but “enabled” by the developmental program<sup>15</sup>. The diameters of 1° and 2° veins are expected to scale positively with leaf length and area, because a greater leaf length expansion rate or duration enables greater vein diameter growth. Similarly, a positive scaling of 1° and 2° vein xylem conduit diameters with vein diameter is enabled by the greater vein expansion in larger leaves.

Minor veins differ from major veins in their predicted scaling with leaf size across species. As minor veins are initiated at the developing leaf tip, greater length expansion provides more space and time for initiating additional minor veins, and thus minor VLA would scale positively with final leaf length. However, as minor veins are initiated later during leaf width expansion, and their diameter growth and spacing is more limited, their vein traits would be independent of final width. The positive scaling of minor VLA with leaf length and its decoupling from leaf width would result in a weak positive scaling of minor VLA with leaf area. Total VLA, i.e., summing major and minor veins, would be decoupled from leaf area, due to the negative scaling of major VLA with leaf width and the positive scaling of minor VLA with leaf length. Additional scaling predictions arise from the scaling of vein diameters and lengths with leaf size (Supplementary Table 6). Like major vein diameters, vein surface and projected areas and volumes per leaf area (VSA, VPA and VVA, respectively) would scale positively with leaf length, and, like major VLA, negatively with leaf width. These counteracting trends lead to predictions that VSA, VPA and VVA are decoupled from leaf area.

The developmental model predicts that grass species with smaller leaf dimensions would develop vein traits conferring stress tolerance, including narrower major veins and higher major VLA, VSA, VPA and VVA, which contribute to water transport efficiency and lower vulnerability to cold and drought<sup>5,6</sup> (Fig. 1a, Supplementary Table 4). Yet, large grass leaves can attain high minor and total VLA, VSA, VPA and VVA, independently of leaf size, enabling high transport efficiency to compete in sunny, moist climates.

C<sub>3</sub> and C<sub>4</sub> species were predicted to converge in their vein scaling. C<sub>4</sub> grasses have higher total VLA, providing a large vein bundle sheath compartment for concentrating CO<sub>2</sub> to enable high rates of photosynthetic assimilation<sup>15-17</sup>. We hypothesized the high total VLA of C<sub>4</sub> grasses arises from minor VLA, and therefore independently of leaf area.

## 68 **Relationship of leaf size with climate**

69 Globally, grasses vary by more than 625-fold, 275-fold, and 160,000-fold in leaf length, width  
70 and area respectively<sup>8,18</sup> and smaller leaves are associated with cooler and drier climates (Fig. 1b,  
71 1c; Supplementary Tables 1-2, 7). Across species, leaf length, width and area were inter-related,  
72 and all were positively correlated with mean annual temperature (MAT), mean annual  
73 precipitation (MAP), and aridity index (AI) (for leaf area,  $r = 0.24-0.31$ ,  $P < 0.001$ ; phylogenetic  
74  $r = 0.08-0.17$ ,  $P < 0.001$ ; Fig. 1c, Extended Data Fig. 2, Supplementary Table 7). Similar  
75 relationships were found with growing season temperature and precipitation (GST and GSP,  
76 respectively) and growing season length (Supplementary Table 7). The climatic associations of  
77 smaller leaves were independent of plant stature, and statistically similar for C<sub>3</sub> and C<sub>4</sub> species  
78 (Supplementary Tables 7-8). Grass leaf size was associated interactively with MAT and MAP,  
79 and with GST and GSP (Extended Data Fig. 3, Supplementary Table 8). The climatic  
80 distribution of grass leaf size arises at least in part from exclusion of large-leafed species from  
81 dry and cold climates (Extended Data Fig. 4, Supplementary Table 8).

82

## 83 **Thermal benefits of small leaf size**

84 We tested three hypotheses for thermal advantages of small leaves for grasses in cold and dry  
85 climates using heuristic energy budget modeling<sup>19,20</sup>. First, small leaves may avoid chilling or  
86 overheating damage, a mechanism that explains the global biogeographic trend in eudicot leaf  
87 size<sup>3</sup>. However, 98% of grass species in the global database had leaves smaller than modelled  
88 width thresholds for such damage, i.e., 8.16 and 4.47 cm, respectively<sup>3</sup> and among these species  
89 leaf size remained associated with climate (Extended Data Fig. 5), indicating that this  
90 mechanism cannot explain the global trend. Second, small leaves, being better coupled with air  
91 temperature, may achieve higher light-saturated photosynthetic rate (A) or leaf water use  
92 efficiency (WUE) under cold or dry climates<sup>20</sup> (Supplementary Table 9; Extended Data Fig 5).  
93 These benefits were supported by model simulations, especially at slower wind speeds;  
94 comparing the 5<sup>th</sup> with the 95<sup>th</sup> percentile of leaf sizes in our global database, the smaller leaves  
95 had 9-27% higher A and/or WUE under cold or dry climates (Supplementary Table 9). Third,  
96 smaller leaves may mitigate the short daily and/or seasonal growth period associated with cold  
97 and dry regions with a higher A under warm and moist conditions<sup>4</sup>, a benefit supported by our

98 simulations, which also showed that smaller leaves had higher transpiration rates (Supplementary  
99 Table 9).

100

### 101 **Developmental scaling of grass venation**

102 Developmental vein scaling results in strong association of vein traits with grass leaf size. As  
103 predicted, globally, smaller leaved species had higher major VLA ( $r = -0.84$  to  $-0.75$ ,  $P < 0.001$ ;  
104 Fig. 1d, Extended Data Fig. 6). For the 27 grass species grown in the common garden,  
105 developmental scaling was supported over the null hypothesis of geometric scaling for numerous  
106 vein traits (91 versus 27 of the 111 scaling predictions;  $P < 0.001$ ; proportion test; Figs. 2-3,  
107 Table 1, Extended Data Figs. 6-7, Supplementary Tables 10-11). The diameters of 1° and 2°  
108 veins scaled positively with leaf length and area ( $b = 0.32$ - $0.37$ ;  $r = 0.61$ - $0.76$ ;  $P < 0.001$ ; Fig. 2,  
109 Extended Data Fig. 6), and the diameters of xylem conduits scaled with their vein diameters ( $b =$   
110  $1.3$ - $1.5$ ;  $r = 0.48$ - $0.65$ ,  $P < 0.05 - 0.001$ ; Extended Data Fig. 6). The 1° VLA decreased  
111 geometrically with increasing leaf width and area ( $b = -1.0$  and  $-0.56$  respectively;  $r = -1.00$  and  $-$   
112  $0.61$ ,  $P < 0.001$ ), whereas the 2° VLA decreased less steeply ( $b = -0.62$  and  $-0.31$ ;  $r = -0.82$  and  $-$   
113  $0.46$ ,  $P < 0.05$ ; Fig. 2, Extended Data Fig. 6), and the major and total VLA scaled negatively  
114 with leaf width ( $b = -0.67$  and  $-0.32$ ;  $r = -0.87$  and  $-0.56$ ,  $P < 0.01$ ). The diameters of minor veins  
115 were independent of leaf length, width and area. The predicted trends of 3° and 4° VLA with leaf  
116 length were not significant, but their sum, the total minor VLA, scaled positively with leaf length  
117 ( $b = 0.35$ - $0.36$ ;  $r = 0.56$ - $0.57$ ,  $P < 0.01$ ), and was independent of leaf width and area. The vein  
118 surface area, projected area and volume per leaf area (VSA, VPA and VVA respectively) also  
119 scaled positively with leaf length, and negatively with leaf width, with the exception of only 3°  
120 VVA, and all were independent of leaf area (Extended Data Fig. 7). Beyond the predictions of  
121 the developmental model, the 5° VLA, VSA and VPA scaled positively with leaf width ( $r =$   
122  $0.46$ - $0.57$ ,  $P < 0.05$ ).

123 C<sub>3</sub> and C<sub>4</sub> grasses converged in vein scaling (Fig. 2, Extended Data Fig. 8, Supplementary  
124 Table 3). C<sub>4</sub> species had more numerous, narrower 3° veins with higher VLA, VSA and VPA,  
125 and 7/16 of the C<sub>4</sub> species had 4° veins, resulting in C<sub>4</sub> species having on average almost double  
126 the total VLA of the C<sub>3</sub> species. The C<sub>4</sub> species also had narrower 5° veins with lower VSA,  
127 VPA, and VVA ( $P = 0.001 - 0.05$ ).

128

## 129 **Hydraulic benefits of small leaf size**

130 Across the 27 grass species grown experimentally, a number of key vein traits were related to  
131 species' native climates. Small leaf size and higher major VLA, VSA, VPA and VVA were  
132 associated with lower MAP, AI, GSP, and GSL (Supplementary Table 7). Further, tests  
133 supported the assumptions based on the published literature (Supplementary Table 4) that C<sub>3</sub>  
134 grasses adapted to colder or drier climates have higher light-saturated photosynthetic rates in  
135 moist soil, associated with their major vein traits (Extended Data Fig. 9)

136 Developmental scaling would contribute mechanistically to climate adaptation. Globally,  
137 vein scaling trends can explain the absence of leaves larger than 51.4 cm<sup>2</sup> where MAT < 0 °C  
138 (Extended Data Fig. 5), as their midrib conduits would be wider than 35 μm (Extended Data Fig.  
139 6), and thereby vulnerable to freeze-thaw embolism<sup>21</sup>. The narrow xylem conduits of small  
140 leaves would protect against embolism during drought, and their higher major VLA provides a  
141 high capacity flow around blockages, further reducing hydraulic vulnerability to dehydration  
142 (Supplementary Table 4)<sup>6,22-25</sup>. The higher major VLA of smaller leaves would also contribute to  
143 mitigating shorter growing periods associated with colder, drier climates<sup>11,12</sup>, by providing higher  
144 hydraulic conductance, enabling the maintenance of open stomata for higher photosynthetic rate  
145 despite the higher transpiration loads expected from their thinner boundary layer (Extended Data  
146 Fig. 9)<sup>6,26</sup>.

147

## 148 **Discussion**

149 The worldwide association of small grass leaf size with cold and arid climates arises from  
150 millions of years of grass migration and evolution, from the tropics to colder, drier climates and  
151 from forest understoreys to open grasslands<sup>8</sup> (Supplementary Table 1). The biophysical and  
152 developmental advantages of small grass leaves can explain this pattern. The thinner boundary  
153 layer of small grass leaves confers moderately higher photosynthetic rate and water use  
154 efficiency in cold and dry climates, and can mitigate shorter growing days and seasons,  
155 especially under the very low wind speeds expected for closed, dense stands<sup>27-30</sup>. Their higher  
156 major VLA and narrower xylem conduits directly contribute to cold and drought tolerance. The  
157 strong climatic association of leaf size and vein traits indicates a substantial importance against  
158 the background of other adaptations, including leaf hairs, leaf rolling and mesophyll desiccation



159 tolerance, and beyond leaves, annual vs. perennial life history, stem and root hydraulic  
160 adaptation, and root morphology<sup>31-33</sup>.

161 Developmentally-based vein scaling relationships held strongly across diverse grass  
162 species, even including those possessing a pseudopetiole, such as bamboos. These relationships  
163 may also apply to nongrass species from other families within the Poales. Grass developmental  
164 vein scaling relationships were distinct though analogous to those of typical eudicot leaves (Box  
165 1, Figs. 1-2). In eudicots, as expected from their diffuse lamina growth, major vein traits scale  
166 negatively with final leaf area (Supplementary Table 4), whereas in grasses, vein traits scale  
167 more directly with length or width (Box 1, Table 1, Fig. 2). Yet, for both grasses and eudicots,  
168 total VLA, a key determinant of hydraulic capacity and photosynthetic rate<sup>6</sup>, was independent of  
169 final leaf area. This lack of constraint on total VLA would enable grass diversification in leaf  
170 size across environments as for eudicots<sup>5,26,34</sup>, as large-leafed grasses, despite their low major  
171 VLA, can achieve sufficient hydraulic capacity with their minor vein length to occupy wet,  
172 sunny habitats<sup>6, 34,35</sup>. The decoupling of total VLA from leaf size also enables C<sub>4</sub> species to  
173 achieve higher VLA than C<sub>3</sub> species, irrespective of leaf size (Box 1, Fig. 2). However, unlike  
174 eudicots<sup>5</sup>, in grasses, larger leaves did not have higher VVA, a trait that contributes substantially  
175 to leaf construction cost<sup>36</sup>, indicating less restriction on their leaf size evolution in resource-rich  
176 environments, where larger leaves may confer advantages in light-use efficiency, and by shading  
177 other species<sup>37,38</sup>. While the common developmental program across species explains many vein  
178 scaling relationships, these may also arise from selection based on function. In longer leaves,  
179 larger diameter veins may provide necessary structural and hydraulic support<sup>6,39</sup>. In wider leaves,  
180 more numerous 5° transverse veins may reinforce against bending<sup>40</sup>, and provide hydraulic  
181 pathways mitigating their lower major VLA<sup>6</sup>. Similarly, the greater 5° vein diameters in C<sub>3</sub> than  
182 C<sub>4</sub> species may compensate for their lower minor VLA (Fig. 2).

183 The relationships of grass leaf size and vein traits to climate have diverse potential  
184 applications. In eudicots, these traits are frequently included for estimating species' adaptation to  
185 climate<sup>6</sup>, an approach that can be extended to grasses. For grasses, as shown for eudicots<sup>5,41</sup>, vein  
186 scaling can enable the reconstruction of leaf size fossilized leaf fragments, improving  
187 paleoclimate estimation (Extended Data Fig. 10). Anticipating future climate change, leaf size  
188 and vein traits can be key targets for grass crop design, which is central to food and biofuel  
189 security<sup>42,43</sup>. A current grand challenge is the engineering of C<sub>4</sub> metabolism into C<sub>3</sub> crops such as

190 rice<sup>43</sup>, and a higher total VLA has been targeted as a promising step<sup>44,45</sup>. Global trends indicate  
191 that C<sub>4</sub> species with narrow leaves and high major VLA would be especially advantaged under  
192 the increased temperature and irregular precipitation expected for grasslands<sup>25,46,47</sup>.

193

## 194 **References**

195

- 196 1 Hort, A. *Enquiry into plants, vol. I, by Theophrastus*. (Harvard University Press, 1948).
- 197 2 Peppe, D. J. et al. Sensitivity of leaf size and shape to climate: global patterns and  
198 paleoclimatic applications. *New Phytol.* **190**, 724-739 (2011).
- 199 3 Wright, I. J. et al. Global climatic drivers of leaf size. *Science* **357**, 917-921 (2017).
- 200 4 Gates, D. M. Transpiration and leaf temperature. *Ann. Rev. Plant Physio.* **19**, 211-238  
201 (1968).
- 202 5 Sack, L. et al. Developmentally based scaling of leaf venation architecture explains  
203 global ecological patterns. *Nat. Commun.* **3**, 1-10 (2012).
- 204 6 Sack, L. & Scoffoni, C. Leaf venation: structure, function, development, evolution,  
205 ecology and applications in the past, present and future. *New Phytol.* **198**, 983-1000  
206 (2013).
- 207 7 Beer, C. et al. Terrestrial gross carbon dioxide uptake: Global distribution and covariation  
208 with climate. *Science* **329**, 834-838 (2010).
- 209 8 Gallaher, T. J. et al. Leaf shape and size track habitat transitions across forest-grassland  
210 boundaries in the grass family (*Poaceae*). *Evolution* **73**, 927-946 (2019).
- 211 9 Soreng, R. J. et al. A worldwide phylogenetic classification of the *Poaceae* (Gramineae)  
212 II: An update and a comparison of two 2015 classifications. *J. Syst. Evol.* **55**, 259-290  
213 (2017).
- 214 10 Schuepp, P. H. Tansley review No. 59 Leaf boundary layers. *New Phytol.* **125**, 477-507  
215 (1993).
- 216 11 Oriens, G. H. & Solbrig, O. T. A cost-income model of leaves and roots with special  
217 reference to arid and semiarid areas. *Am. Nat.* **111**, 677-690 (1977).
- 218 12 Körner, C. Plant adaptation to cold climates. *FI000 Research* **5**, 1-5 (2016).
- 219 13 Niklas, K. J. *Plant Allometry: the scaling of form and process*. (University of Chicago  
220 Press, 1994).

- 221 14 Nelson, T. & Dengler, N. Leaf vascular pattern formation. *Plant Cell* **9**, 1121-1135  
222 (1997).
- 223 15 Christin, P. A. et al. Anatomical enablers and the evolution of C<sub>4</sub> photosynthesis in  
224 grasses. *P. Natl. Acad. Sci. USA* **110**, 1381-1386 (2013).
- 225 16 Ueno, O., Kawano, Y., Wakayama, M. & Takeda, T. Leaf vascular systems in C<sub>3</sub> and C<sub>4</sub>  
226 grasses: A two-dimensional analysis. *Ann. Bot-London* **97**, 611-621 (2006).
- 227 17 Sage, R. F. The evolution of C<sub>4</sub> photosynthesis. *New Phytol.* **161**, 341-370 (2004).
- 228 18 Clayton, W. D., Vorontsova, M. S., Harman, K. T. & Williamson, H. *GrassBase - The*  
229 *Online World Grass Flore*, <<http://www.kew.org/data/grasses-db.html>> (2006).
- 230 19 Parkhurst, D. F. & Loucks, O. L. Optimal leaf size in relation to environment. *J. Ecol.* **60**,  
231 505-537 (1972).
- 232 20 Okajima, Y., Taneda, H., Noguchi, K. & Terashima, I. Optimum leaf size predicted by a  
233 novel leaf energy balance model incorporating dependencies of photosynthesis on light  
234 and temperature. *Ecol. Res.* **27**, 333-346 (2011).
- 235 21 Davis, S. D., Sperry, J. & Hacke, U. The relationship between xylem conduit diameter  
236 and cavitation caused by freezing. *Am. J. Bot.* **86**, 1367-1372 (1999).
- 237 22 Blackman, C. J., Brodribb, T. J. & Jordan, G. J. Leaf hydraulic vulnerability is related to  
238 conduit dimensions and drought resistance across a diverse range of woody angiosperms.  
239 *New Phytol.* **188**, 1113-1123 (2010).
- 240 23 Scoffoni, C., Rawls, M., McKown, A., Cochard, H. & Sack, L. Decline of leaf hydraulic  
241 conductance with dehydration: Relationship to leaf size and venation architecture. *Plant*  
242 *Physiol.* **156**, 832-843 (2011).
- 243 24 Scoffoni, C. et al. Leaf vein xylem conduit diameter influences susceptibility to  
244 embolism and hydraulic decline. *New Phytol.* **213**, 1076-1092 (2017).
- 245 25 Craine, J. M. et al. Global diversity of drought tolerance and grassland climate-change  
246 resilience. *Nat. Clim. Change* **3**, 63-67 (2013).
- 247 26 Scoffoni, C. et al. Hydraulic basis for the evolution of photosynthetic productivity. *Nat.*  
248 *Plants* **2**, 1-8 (2016).
- 249 27 Jones, H. G. *Plants and microclimate : a quantitative approach to environmental Plant*  
250 *Physiol.*. Third edition. edn, (Cambridge University Press, 2014).
- 251 28 Grace, J. *Plant-atmosphere relationships*. 1st edn, (Chapman and Hall Ltd, 1983).

252 29 Weiser, R. L., Asrar, G., Miller, G. P. & Kanemasu, E. T. Assessing grassland  
253 biophysical characteristics from spectral measurements. *Remote Sens. Environ.* **20**, 141-  
254 152 (1986).

255 30 Meinzer, F. C. G., D. A. Stomatal control of transpiration from a developing sugarcane  
256 canopy. *Plant Cell Environ.* **12**, 635-642 (1989).

257 31 Liu, H. et al. Life history is a key factor explaining functional trait diversity among  
258 subtropical grasses, and its influence differs between C<sub>3</sub> and C<sub>4</sub> species. *J. Exp. Bot.* **70**,  
259 1567-1580 (2019).

260 32 Fort, F., Jouany, C. & Cruz, P. Root and leaf functional trait relations in *Poaceae* species:  
261 Implications of differing resource-acquisition strategies. *J. Plant Ecol.* **6**, 211-219 (2013).

262 33 Holloway-Phillips, M. M. & Brodribb, T. J. Contrasting hydraulic regulation in closely  
263 related forage grasses: implications for plant water use. *Funct. Plant Biol.* **38**, 594-605  
264 (2011).

265 34 Brodribb, T. J., Feild, T. S. & Sack, L. Viewing leaf structure and evolution from a  
266 hydraulic perspective. *Funct. Plant Biol.* **37**, 488-498 (2010).

267 35 Linacre, E. T. Further notes on a feature of leaf and air temperatures. *Archiv für*  
268 *Meteorologie, Geophysik und Bioklimatologie, Serie B* **15**, 422-436 (1967).

269 36 John, G. P. et al. The anatomical and compositional basis of leaf mass per area. *Ecol.*  
270 *Lett.* **20**, 412-425 (2017).

271 37 Givnish, T. J. Comparative studies of leaf form: Assessing the relative roles of selective  
272 pressures and phylogenetic constraints. *New Phytol.* **106**, 131-160 (1987).

273 38 Lusk, C. H., Grierson, E. R. P. & Laughlin, D. C. Large leaves in warm, moist  
274 environments confer an advantage in seedling light interception efficiency. *New Phytol.*  
275 **223**, 1319-1327 (2019).

276 39 Olson, M. E. et al. Plant height and hydraulic vulnerability to drought and cold. *P. Natl.*  
277 *Acad. Sci. USA* **115**, 7551-7556 (2018).

278 40 Niklas, K. J. A mechanical perspective on foliage leaf form and function. *New Phytol.*  
279 **143**, 19-31 (1999).

280 41 Merkhofer, L. et al. Resolving Australian analogs for an Eocene Patagonian  
281 paleorainforest using leaf size and floristics. *Am. J. Bot.* **102**, 1160-1173 (2015).

282 42 Somerville, C. The billion-ton biofuels vision. *Science* **312**, 1277-1277 (2006).

- 283 43 Sedelnikova, O. V., Hughes, T. E. & Langdale, J. A. Understanding the genetic basis of  
284 C<sub>4</sub> Kranz anatomy with a view to engineering C<sub>3</sub> crops. *Ann. Rev. Gen.* **52**, 249-270  
285 (2018).
- 286 44 Sage, R. F. & Zhu, X. G. Exploiting the engine of C<sub>4</sub> photosynthesis. *J. Exp. Bot.* **62**,  
287 2989-3000 (2011).
- 288 45 Feldman, A. B. et al. Increasing leaf vein density via mutagenesis in rice results in an  
289 enhanced rate of photosynthesis, smaller cell sizes and can reduce interveinal mesophyll  
290 cell number. *Front. Plant Sci.* **8**, 1-10 (2017).
- 291 46 Edwards, E. J. et al. The origins of C<sub>4</sub> grasslands: Integrating evolutionary and ecosystem  
292 science. *Science* **328**, 587-591 (2010).
- 293 47 Linder, H. P., Lehmann, C. E. R., Archibald, S., Osborne, C. P. & Richardson, D. M.  
294 Global grass (*Poaceae*) success underpinned by traits facilitating colonization,  
295 persistence and habitat transformation. *Biol. Rev.* **93**, 1125-1144 (2018).

296  
297  
298  
299

### 300 Main Figure/Display Legends

301

#### 302 Fig. 1. Relationships of grass leaf size, traits and species' climatic distribution worldwide.

303 (a) Linkages of small leaf size with traits, adaptation to cold and dry climates, and biogeography,  
304 as established for eudicotyledons (Supplementary Table 4), and hypothesized for grasses. Small  
305 leaves have thin boundary layers (BL), and develop lower major vein diameters (VD<sub>major</sub>), and  
306 higher major vein length per area (VLA<sub>major</sub>), which provide advantages in cold or dry climates  
307 (Supplementary Table 4). Large leaves would be disadvantaged in such climates, relative to  
308 warm and moist climates. (b) Grass leaf area averaged per country in the global database (across-  
309 species mean of leaf area for 21 to 547 species per country; gray when < 20 species represented).  
310 (c) Grass leaf area in relation to aridity index (where low index signifies a drier climate); each  
311 point represents a species ( $n = 912$  C<sub>3</sub> and 840 C<sub>4</sub> species respectively); contour lines and colors  
312 represent the 2d kernel density of points. (d) The association of major vein length per area  
313 (VLA<sub>major</sub>) with leaf area across grass species ( $n = 600$  species). Statistics represent the fits for

314  $\log(y) = \log(a) + b \log(x)$  from ordinary least squares in (c) and (d).  $P =$  (c)  $2.3 \times 10^{-27}$  and (d)  
315  $1.6 \times 10^{-139}$  (both two-tailed).

316

317 **Fig. 2. The scaling of vein traits with leaf dimensions for 27 species of C<sub>3</sub> and C<sub>4</sub> grasses**  
318 **grown in a common garden. (a) – (d)** Relationships of vein diameters with leaf length and (e) –  
319 (h) of vein lengths per unit leaf area with leaf width: (a) & (e) first order (1°) veins (b) & (f)  
320 second order (2°) veins (c) & (g) third order (3°) veins, and, for the species that possess them,  
321 fourth order (4°) veins (inset panels) and (d) & (h) fifth order (5°) transverse veins. Each point  
322 represents a species mean value (n = 11 C<sub>3</sub> in white and n = 16 C<sub>4</sub> in gray). Reduced major axis  
323 (PRMA) or phylogenetic generalized least square regressions were fitted for  $\log(\text{vein diameter}$   
324  $\text{or vein length per area}) = \log(a) + b \log(\text{leaf length or width})$ , respectively; parameters and  
325 goodness of fit in Table 1 and Supplementary Table 10.  $**P < 0.01$ ,  $***P < 0.001$ ;  $P =$  (a)  
326 0.0007, (b)  $3.9 \times 10^{-6}$ , (e)  $1.2 \times 10^{-34}$ , (f)  $1.4 \times 10^{-7}$  and (h) 0.0020 (all two-tailed). Significant  
327 trends are plotted with PRMA. Standard errors for species trait values are found in  
328 Supplementary Table 3.

329

330 **Box 1 Fig. 1 Synthetic model for grass leaf ontogeny predicting developmentally-based**  
331 **scaling of vein traits with final leaf size across species.** Processes are plotted against  
332 developmental phases: phases P and D, formation of the leaf primordium and the cell division  
333 zone at the base of the leaf (DZ), respectively; phases D-E and D-E-M, the additions of the  
334 expansion zone (EZ) and the maturation zone, respectively; and phase M, maturation of the  
335 whole leaf blade. (a) Leaf expansion and the formation of zones; (b) Increases of leaf length,  
336 width and area; (c) Patterning of leaf vein orders from 1° veins to 5° transverse veins for C<sub>3</sub> and  
337 C<sub>4</sub> species; some C<sub>4</sub> species develop 4° longitudinal veins (C<sub>4-4L</sub> species), whereas C<sub>3</sub> species  
338 and C<sub>4-3L</sub> species do not; (d) Increases in vein length per leaf area and (e) in vein diameter for  
339 each vein order.

340

341 **Table 1. Parameters for the scaling of vein diameters and vein lengths per area with**  
342 **mature leaf dimensions across 27 C<sub>3</sub> and C<sub>4</sub> grass species grown in a common garden (N =**  
343 **11 and 16 respectively).** Tolerance of cold or dry climates can be conferred by these vein traits  
344 and others (vein surface area per leaf area, projected area per leaf area and volume per leaf area,

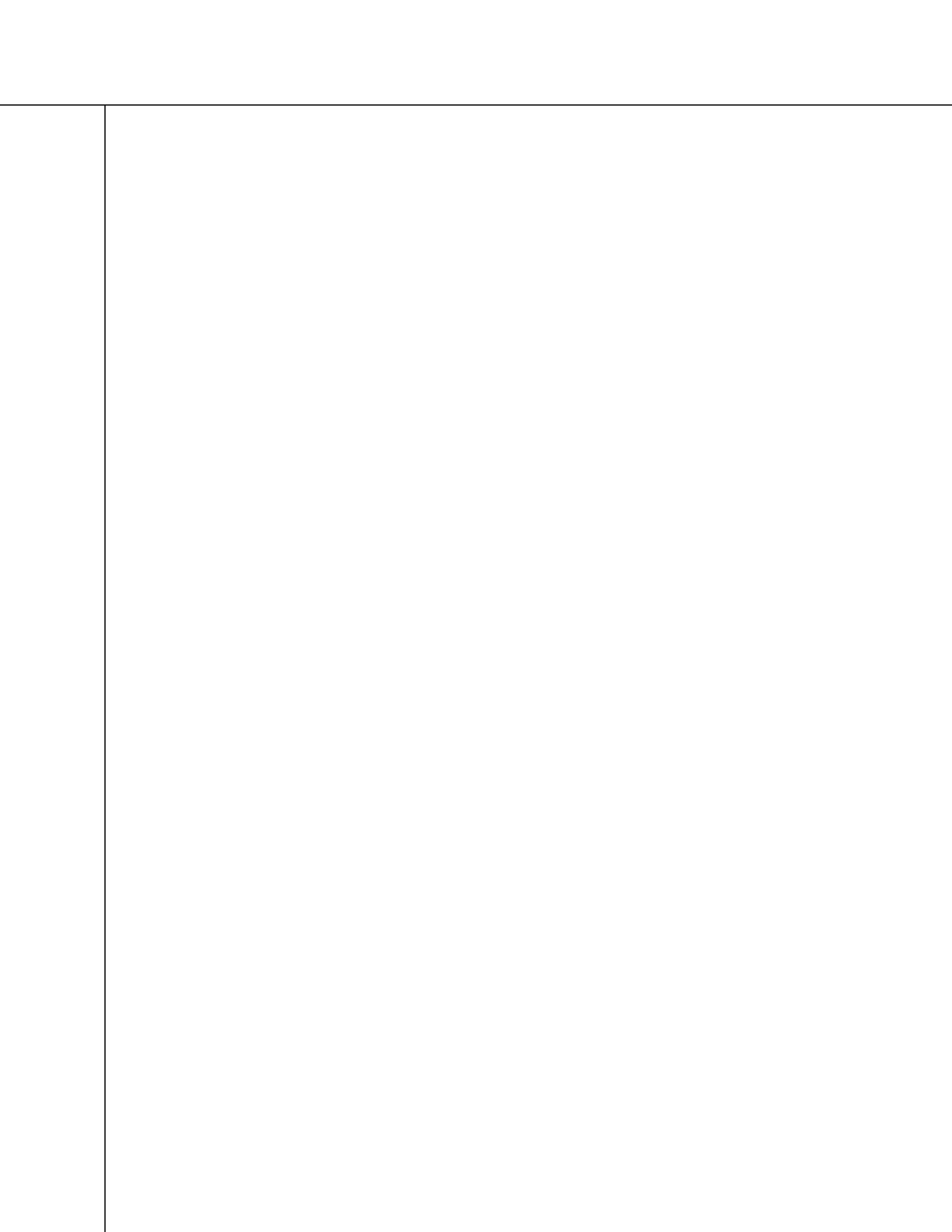
345 shown in Supplementary Table 10), as they influence hydraulic capacity and safety, and vascular  
346 cost (Supplementary Table 4). Expectations for these across-species scaling relationships were  
347 derived from a developmental model, which predicts the allometric slope  $b$  in the equation  $\log$   
348 (trait) =  $\log(a) + b \log(\text{mature leaf length, width or area})$  (Supplementary Table 6), due to  
349 intrinsic ( $i$ ) and enabling ( $e$ ) effects (Box 1); expectations from the alternative, geometric scaling  
350 model were also derived (Supplementary Tables 6 and 10). Allometric equations were fitted  
351 using two-tailed phylogenetic reduced major axis (PRMA) or phylogenetic generalized least  
352 squares (PGLS) for the scaling of vein diameter or vein length per area, respectively, with  $r$ -  
353 values and  $p$ -values, and parameters  $a$  and  $b$ , including 95% confidence intervals (CIs) for  $b$ -  
354 values. Bold type indicates that the  $b$ -values predicted from the developmental model were  
355 supported in the experimental, i.e., the scaling relationship across species was significant, and the  
356 predicted  $b$ -value was within the 95% CIs for the observed  $b$ -value. Significance: \* $P < 0.05$ , \*\* $P$   
357  $< 0.01$ , \*\*\* $P < 0.001$ , NS: Not significant.

358

359

360

361





363 **Methods**

364 **Testing for the linkage of leaf size and vein traits with climate across grass species**

365 **worldwide**

366 We extracted data from the Kew Royal Botanic Garden Grassbase, which was compiled from a  
367 combination of floristic accounts and publications<sup>18</sup>. We extracted all available data for  
368 maximum leaf length, maximum leaf width, maximum 2° vein number, and maximum culm  
369 height data, which included values for up to 1752 species depending on the trait (i.e., up to 912  
370 C<sub>3</sub> and 840 C<sub>4</sub> species from 373 genera)<sup>18</sup>. We calculated leaf area by multiplying maximum leaf  
371 length by maximum leaf width. We divided the maximum leaf length and maximum 2° vein  
372 number respectively by maximum leaf width to determine 1° and 2° vein lengths per area, and  
373 summed these to calculate major vein length per area, resulting in values for 616 species for  
374 these traits. To test associations of leaf morphological and venation traits with species' native  
375 climates, we extracted geographical records from the Global Biodiversity Information Facility  
376 web portal (<http://www.gbif.org>). Species names were checked against the Kew grass synonymy  
377 database<sup>18</sup> via the software package Taxonome<sup>48</sup> and The Plant List (<http://www.theplantlist.org>)  
378 via package Taxostand in R<sup>49</sup>. We discarded records if these were duplicates, or names were not  
379 recognized in any databases, or the country did not match the coordinates, or coordinates  
380 contained fewer than three decimals, or species had fewer than five occurrences. For each  
381 location, values for mean annual temperature (MAT), mean annual precipitation (MAP), and  
382 mean monthly temperature and precipitation were extracted from WorldClim2 5-arc minute  
383 resolution<sup>50</sup>, and for aridity index (AI)<sup>51</sup> from CRU TS4.01 01<sup>52</sup>. We also estimated growing  
384 season variables, considering growing season months as those with mean temperature  $\geq 4$  °C and  
385 precipitation  $\geq 2 \times$  mean monthly temperature; growing season length (GSL) was calculated as  
386 the number of those months, growing season temperature (GST) by averaging their mean  
387 temperatures, and growing season precipitation (GSP) by summing their mean precipitation<sup>53</sup>.  
388 Climate variables were averaged from all given locations for each species. We focused on the  
389 relationships of traits with mean climate variables based on the hypothesis that if gene flow  
390 occurs among populations of a given species across its native range, that species' mean  
391 phenotypic trait values would be related to their mean climate variables<sup>54</sup>.

392

393 **Construction of a synthetic model for grass leaf development, and derivation of allometric**  
394 **predictions based on developmental and geometric scaling**

395 To determine whether leaf development would constrain specific vein traits in smaller leaves, we  
396 formulated a synthetic grass leaf developmental model and derived expectations for the  
397 relationship of vein traits with final leaf dimensions across species (Box 1, Supplementary  
398 Tables 5-6). To construct this model, we conducted searches for previously published studies  
399 that included developmental data and/or images of grass leaf development using the keywords  
400 “grass leaf development”, “grass vein development”, “grass histogenesis”, “grass  
401 morphogenesis”, “Poaceae”, “leaf ontogeny”, “leaf histology”, “leaf growth”, “leaf anatomy”,  
402 “vascular development”, “vasculature development” in the Web of Science database and the  
403 Google Scholar search engine, resulting in a compilation of 61 studies of 20 grass species<sup>14,55-114</sup>.  
404 From these studies we extracted key steps in leaf and vein development that were general across  
405 species into a synthetic model. Then, given the spatial and temporal constraints arising from  
406 development according to this model, we derived expectations for the scaling across species of  
407 vein traits with mature leaf size. For instance, the 1° vein length per area declines geometrically  
408 with final leaf width (1° VLA = 1/leaf width) as veins are separated by greater numbers of cell  
409 divisions and/or by larger cells. By contrast, the 2° VLA declines less steeply than geometrically  
410 with final leaf width, as wider leaves may form greater numbers of 2° veins though these will be  
411 spaced further apart by subsequent leaf expansion (see Box 1 and Supplementary Table 6 for  
412 additional derivations).

413 Further, as a null hypothesis against which to test developmentally-based scaling  
414 predictions, we derived expectations for the relationships of vein traits to leaf dimensions based  
415 on geometric scaling<sup>5,13</sup>. Geometric scaling represents the relationships expected among the  
416 dimensions of an object given increases in size while maintaining constant proportions and  
417 composition. Thus, linear dimensions such as length ( $L$ ), area ( $A$ ) and volume ( $V$ ) would be inter-  
418 related as  $A \propto L^2$  and  $V \propto L^3$ . Predictions can then be derived for any other traits based on their  
419 dimensions. For instance, given geometric scaling, VLA would be expected to scale with leaf  
420 width as  $VLA \propto LW^{-1}$ , because VLA, as a linear dimension divided by an area, i.e.,  $L/A$ , would  
421 be related to  $L/L^2$ , =  $L^{-1}$ , whereas  $LW$  would scale directly with  $L$ . In total, 111 predictions  
422 derived from the developmental model were compared with respective predictions from  
423 geometric scaling. These 111 predictions included the scaling relationships of five vein

424 diameters (i.e., for each of five vein orders) versus three leaf dimensions (i.e., leaf length, width  
425 and area), amounting to 15 predictions; plus the scaling relationships for VLA, VSA, VPA and  
426 VVA for each of the five vein orders and for the major, vein, and total vein systems, versus the  
427 three leaf dimensions, amounting to  $4 \times 8 \times 3 = 96$  predictions. The developmental model  
428 predictions for relationships generally differed strongly from those of geometric scaling (i.e.,  
429 75% of predictions differed), though, for a few relationships, such as that of 1<sup>o</sup> VLA with final  
430 leaf size, the expectations from developmental scaling and geometric scaling were the same.  
431 Overall, developmental scaling predicted that 51 vein traits would scale with leaf size and 60  
432 traits would be independent of leaf dimensions, whereas geometric scaling predicted 63 and 48  
433 respectively (Supplementary Table 6 and 10).

434

### 435 **Plant material**

436 To test vein scaling relationships, grasses of 27 diverse species were grown in a common garden  
437 to reduce the environmentally-induced plasticity that would occur in wild plants in their native  
438 ranges (Extended Data Fig. 2, Supplementary Table 3). While experimental species were  
439 selected to encompass large phylogenetic and functional variation, including 11 C<sub>3</sub> species and  
440 16 C<sub>4</sub> species, representing 11 independent C<sub>4</sub> origins, the species necessarily included a only  
441 subset of the phylogenetic distribution of the 1752 species in the database analyses of global  
442 trait-climate relationships. Seeds were acquired from seed banks and commercial sources  
443 (Supplementary Table 3). Prior to germination, seeds were surface-sterilized with 10% NaClO  
444 and 0.1% Triton X-100 detergent, rinsed three times with sterile water, and finally sown on  
445 plates of 0.8 % agar sealed with Micropore surgical tape (3M, St. Paul, MN). Seeds were  
446 germinated in chambers maintained at 26°C, under moderate intensity cool white fluorescent  
447 lighting with a 12 hour photoperiod. When roots were 2-3 cm long, seedlings were transplanted  
448 to 3.6 L pots with potting soil (1:1:1.5:1.5:3 of coarse vermiculite: perlite: washed plaster sand:  
449 sandy loam: peat moss).

450 Plants were grown at the UCLA Plant Growth Center (minimum, mean and maximum  
451 daily values for temperature: 20.1, 23.4 and 34.0 °C; for relative humidity: 28, 50 and 65%; and  
452 mean and maximum photosynthetically active radiation during daylight period: 107 and 1988  
453  $\mu\text{mol photons m}^{-2} \text{ s}^{-1}$ ; HOBO Micro Station with Smart Sensors; Onset, Bourne, MA), arranged  
454 in six randomized blocks spread over three benches, with one individual per species per block

455 and two blocks per bench ( $n = 6$  except  $n = 4$  for *Alloteropsis semialata*). Plants were irrigated  
456 daily with water containing fertilizer (200-250 ppm of 20:20:20 N:P:K; Scotts Peters  
457 Professional water soluble fertilizer; Everris International B.V., Geldermalsen, The Netherlands).  
458 All species were grown until flowering to confirm species' identities.

459

#### 460 **Sample anatomical preparation**

461 Leaves were collected when plants had numerous mature leaves, after 2.5 – 7 months of growth,  
462 depending on species, given variation in growth rates. Leaves from each of six individuals per  
463 species were fixed and stored in FAA solution (37% formaldehyde-glacial acetic acid-95%  
464 ethanol in deionized water). Transverse sections were made for one leaf from each of three  
465 individuals. Rectangular samples were cut from the center of leaves halfway along the length of  
466 the blade and gradually infiltrated under vacuum with low viscosity acrylic resin for one week  
467 (L.R. White; London Resin Co., UK), and set in resin in gelatin capsules to dry at 55 °C  
468 overnight. Transverse cross sections 1  $\mu\text{m}$  in thickness were prepared using glass knives (LKB  
469 7800 KnifeMaker; LKB Produkter; Bromma, Sweden) in a rotary microtome (Leica Ultracut E,  
470 Reichert-Jung California, USA), placed on slides, and stained with 0.01% toluidine blue in 1%  
471 sodium borate (w/v). Slides were imaged with a light microscope using a 5 $\times$ , 20 $\times$ , and 40 $\times$   
472 objective (Leica Lietz DMRB; Leica Microsystems) and camera with imaging software (SPOT  
473 Imaging Solution; Diagnostic Instruments, Sterling Heights, Michigan USA). Additionally, one  
474 leaf from each of three individuals was used to prepare chemically cleared leaf sections to  
475 visualize veins. Square sections of 1 cm  $\times$  1 cm were cut from the center of the leaf at the widest  
476 point, cleared with 5 % NaOH in ethanol, stained with safranin, and counterstained with fast-  
477 green<sup>115</sup>. Sections were mounted with water in transparency film (CG5000; 3M Visual Systems  
478 Division) and scanned (flatbed scanner; Canon Scan Lide 90; 1,200 pixels per inch), and further  
479 imaged with a light microscope using a 5 $\times$  and 10 $\times$  objective.

480

#### 481 **Quantification of leaf dimensions and vein traits**

482 Leaf dimensions tested were leaf width, leaf length, and leaf area, with leaf width and leaf length  
483 measured at the widest and longest regions of the leaf respectively. Leaf area was calculated as  
484 leaf length  $\times$  leaf width<sup>116-118</sup>. Estimates of leaf area from length and width can be improved by  
485 multiplying by a correction factor constant, which has been proposed as 0.7-0.9 for grasses<sup>116-118</sup>,

486 but as there is no standard value, we did not apply such a correction factor. Applying a constant  
487 correction factor would have no influence on correlations or regression fits or their statistical  
488 significance for trait-climate relationships. Further, applying a constant correction factor would  
489 not influence the tests of scaling of vein traits with leaf area, which focused on power law scaling  
490 exponents; multiplying estimates of leaf area by a constant would result only in change to the  
491 power law scaling intercept, and not the exponent. Thus, applying a correction factor to leaf area,  
492 or not, would have no influence any of the findings of our study.

493 We measured and analyzed cross sections of one leaf for each of three individuals per  
494 species, to quantify the diameters and numbers of veins in the transverse plane for all vein  
495 orders, excluding 5° veins, which generally were not visible in transverse sections, and for which  
496 we used the chemically cleared and stained leaf sections. Vein orders were established for each  
497 species based on vein size, presence/absence of enlarged metaxylem, and presence/absence of  
498 fibrous tissue above or below the vein<sup>119,120</sup>. The 1° vein or midvein was the large central vein  
499 containing the largest metaxylem and fibrous tissue, and the 2° veins were the “large” veins that  
500 were substantially smaller than the midvein and of similar structure. We identified the minor  
501 veins as the smaller veins, i.e., the 3° “intermediate” and 4° “small” veins, and perpendicular 5°  
502 transverse veins<sup>120</sup>. Notably, 4° veins occur only in NADP-ME C<sub>4</sub> grasses of the subfamily  
503 Panicoideae (7/16 of the C<sub>4</sub> species)<sup>15</sup>, and can be distinguished based on their smaller overall  
504 size than 3° veins and their absence of sclerenchyma strands. For the species *Lasiacis*  
505 *sorghoidea*, 2° veins were too few to be counted in our prepared transverse sections, and we  
506 established vein orders and quantified associated traits using the chemically cleared and stained  
507 leaves.

508 For each vein order, the vein length per area (VLA) was quantified as the vein number  
509 per leaf width (cm<sup>-1</sup> or mm<sup>-1</sup>), which is equivalent to vein length per unit leaf area (same units),  
510 assuming an approximately rectangular leaf. Cross-sectional vein diameters (VD) were measured  
511 excluding the bundle and mestome sheath cell layers, and averaging horizontal and vertical axes.  
512 Cross-sectional diameters were measured for all xylem conduits in each vein order by  
513 considering the lumen cross-sections as ellipses and averaging the major and minor axes. We  
514 categorized two metaxylem types within major veins, based on their highly distinct sizes (i.e.,  
515 large and small metaxylem), and one metaxylem type for minor veins (i.e., “small metaxylem”).  
516 We focused on the large metaxylem conduits within major veins in calculating average conduit

517 diameter values, as these would contribute the bulk of maximum flow<sup>121,122</sup>. For *Lasiacis*  
518 *sorghoidea*, as 2° veins were too few to be counted from our prepared transverse sections, we  
519 could not quantify the conduits within these veins and thus analyses of 2° vein conduit  
520 dimensions excluded this species.

521 For all vein orders, we estimated vein surface per unit leaf area (VSA), vein projected  
522 area per unit leaf area (VPA), and vein volume per unit leaf area (VVA)<sup>5</sup>:

523 
$$VSA = VLA \times \pi \times VD \quad (2)$$

524 
$$VPA = VLA \times VD \quad (3)$$

525 
$$VVA = VLA \times \pi \times (VD/2)^2 \quad (4)$$

526

527 **Determination of vein allometries, and testing against predictions from developmental and**  
528 **geometric scaling**

529 We determined trait scaling relationships by fitting lines to log-transformed data. The  
530 relationship of each vein trait (y) to a given leaf dimension (x) was considered as an allometric  
531 power law:

532 
$$y = ax^b \quad (5)$$

533 
$$\log(y) = \log(a) + b \log(x)$$

534 where *b* is the scaling exponent.

535 We tested these relationships against the predictions from developmentally-based scaling  
536 derived from the synthetic leaf developmental model (see “*Construction of a synthetic model for*  
537 *grass leaf development, and derivation of allometric predictions based on developmental and*  
538 *geometric scaling*” and Box 1, Table 1, and Supplementary Table 6)<sup>5</sup>. A scaling relationship was  
539 considered to be consistent with a prediction if its 95% confidence intervals included the  
540 predicted slope. We tested whether a greater proportion of predictions were explained by  
541 developmental scaling than by geometric scaling using a proportion test (Minitab 16; State  
542 College, Pennsylvania, USA).

543

544 **Testing assumptions for the linkages of photosynthetic rate with climate and vein traits**

545 For the grass species grown experimentally, light-saturated rates of photosynthesis were  
546 measured for plants in moist soil, enabling a test of the assumptions that C<sub>3</sub> grass species from  
547 arid or cold environments have high photosynthetic rates, and that photosynthetic rate would be

548 related to vein length and surface area per leaf area. Light-saturated rates of photosynthesis were  
549 measured from 17 Feb to 28 June 2010, between 0900 and 1500, on a mature leaf on each plant  
550 for six plants per species. Measurements were taken of steady state gas exchange (< 2% change  
551 over six minutes) using a LI-6400 XT portable photosynthesis system (LI-COR, Lincoln,  
552 Nebraska, USA). Conditions within the leaf chamber were set to 25°C, with reference CO<sub>2</sub> 400  
553 ppm, and PPF 2000 μmol m<sup>-2</sup> s<sup>-1</sup>, and the relative humidity was 60-80%, resulting in vapor  
554 pressure deficits (VPD) of 0.80-1.6 kPa. Measurements were made on 1-2 leaves from each of 6  
555 plants (except *L. sorghoidea*, 3 leaves from each of two plants). 5-9 leaves per species were  
556 measured, with 6 on average. Leaves were harvested and scanned for leaf area (Canon Scan Lide  
557 90, Canon USA, Lake Success, NY). Leaf-area normalized values were determined for net light-  
558 saturated photosynthetic rate per leaf area ( $A_{\text{area}}$ ).

559 In addition, we tested for even stronger general support of the relationships of  
560 photosynthetic rate with climate variables by combining our data for 8 C<sub>3</sub> terrestrial species with  
561 data for 13 Northern Hemisphere temperate terrestrial C<sub>3</sub> grass species from the GLObal Plant  
562 trait NETwork (GLOPNET) database<sup>123</sup>, for which photosynthesis, latitude and longitude data  
563 for their field site were available (Supplementary Table 12). We extracted climate variables  
564 mean annual temperature (MAT), mean annual precipitation (MAP), and monthly temperature  
565 and precipitation to calculate growing season length (GSL) (see *Testing for the linkage of leaf*  
566 *size and vein traits with climate across grass species worldwide* above for methods of  
567 calculation), based on the latitude and longitude from which each species was measured.

568

### 569 **Phylogenetic reconstruction**

570 A phylogenetic hypothesis for the 27 experimentally grown species considered in this study was  
571 inferred from three markers from the chloroplast genome (*rbcL*, *ndhF* and *trnKmatK*), available  
572 for the exact same accessions in published datasets<sup>124,125</sup>. Each marker was aligned individually  
573 using MUSCLE<sup>126</sup>, and the alignments were manually refined. The total dataset was 6179 bp  
574 long. The program BEAST<sup>127</sup> was used to obtain a time-calibrated phylogeny under a relaxed  
575 clock model with uncorrelated evolutionary rates that follow a log-normal distribution. The  
576 substitution model was set to a general time reversible model with a gamma-shape parameter and  
577 a proportion of invariants. The root of the tree (split of BOP and PACMAD clades) was forced to  
578 follow a normal distribution with a mean of 51.2 Ma and a standard deviation of 0.0001 Ma,

579 based on previous estimates<sup>128</sup>. The addition of phytolith fossils would alter the absolute ages  
580 estimated by molecular dating<sup>129</sup>, but the relative ages would remain unchanged and the  
581 comparative analyses consequently would be unaffected. Two parallel analyses were run for  
582 10,000,000 generations, sampling a tree every 1,000 generations. Median ages across the 18,000  
583 trees samples are a burn-in period of 1,000,000 generations were mapped on the maximum  
584 credibility tree. The burn-in period was largely sufficient for the analysis to reach stability, as  
585 verified with the program Tracer (<http://beadt.bio.ed.ac.uk/Tracer>).

586 Using the R Language and Environment version 3.4.1<sup>130</sup> with the ape R package<sup>131</sup> a  
587 phylogenetic hypothesis for 1752 of the Grassbase species was extracted from a published  
588 phylogeny available through Dryad<sup>132</sup>. The source phylogeny assessed relationships among 3595  
589 species using a set of 14 sub trees using various genetic datasets in combination with three core  
590 plastid markers *rbcL*, *ndhF* and *matK*, with dating based on macrofossil evidence<sup>9</sup>.

591

## 592 **Testing trait-climate associations**

593 To test trait-climate associations, we quantified the strength of correlations using Pearson  $r$  rather  
594 than fitting specific predictive regression equations with  $R^2$  values. For trait-climate associations  
595 we calculated both ahistorical correlations and relationships accounting for phylogenetic  
596 relatedness (PGLS or PRMA, see section *Comparative analyses* below). While the phylogenetic  
597 analyses more robustly test our evolutionary hypotheses, the ahistorical Pearson  $r$  values better  
598 resolve the strengths of existing relationships across species, especially when trends arise from  
599 variation among groups that split in evolution deep in the phylogeny<sup>133</sup>. In both types of analysis,  
600 the  $r$  values provide a conservative estimate of trait-climate relationships. As in previous  
601 biogeographic trait-climate analyses<sup>134,135</sup>, we related species' average trait values from a  
602 database or experimental measurements to modelled native climates based on natural  
603 occurrences; relationships would be yet stronger if traits and climate were matched for individual  
604 plants<sup>136</sup>. Additionally, the modelled native climates do not account for variation to which  
605 species would be adapted in the field in temperature, irradiance and water availability due to  
606 microclimate associated with topography and canopy cover, or soil characteristics; accounting  
607 for this variation would likely improve the strength of trait-climate relationships<sup>136</sup>. Overall,  
608 global associations of traits with climate that were supported by substantial, statistically  
609 significant ahistorical  $r$  values indicate robust, biologically significant relationships, and



610 significant phylogenetic correlations additionally indicate support for the evolutionary  
611 hypotheses<sup>137,138</sup>.

612 We implemented several further analyses to resolve the associations of traits with climate  
613 in the worldwide grass trait database. We conducted phylogenetic multiple regression to test for  
614 significant interactive effects of temperature and precipitation on leaf traits. Models including  
615 MAT and MAP (or GST and GSP) alone or in combination, and including an interaction were  
616 compared using Akaike Information Criterion (AIC)<sup>139</sup>. Prior to phylogenetic multiple regression  
617 analyses, MAP values were divided by 50 to achieve a similar scale of values as MAT, and GSP  
618 values were divided by 100 to achieve a similar scale of values as GST. Plant traits, MAP and  
619 MAT were then log transformed, and MAT and MAP (and GST and GSP) were centered by  
620 subtracting the mean to render coefficients of main effects and interaction terms biologically  
621 interpretable<sup>140</sup>.

622 The parametric correlation and regression statistics calculated in this study are subject to  
623 assumptions, i.e., independence of observations, and the normal distribution and  
624 homoscedasticity of residuals<sup>141</sup>. Evolutionary non-independence among species was adjusted  
625 for using phylogenetic statistics<sup>133</sup>. To check that the assumptions of normality and  
626 heteroscedasticity did not influence statistical significance of univariate analyses, we checked for  
627 significance of Spearman's rank correlations, which are not subject to these assumptions, and  
628 confirmed as significant ( $p < 0.05$ ) the relationships presented in the text. For the multiple  
629 regression of leaf area versus MAT and MAP in the 1752 species global database, the 29 species  
630 with  $\text{MAT} < 0 \text{ }^\circ\text{C}$  resulted in a left-skew of log-transformed MAT and a notable  
631 heteroscedasticity of residuals (Supplementary Fig. 1). To confirm that this skew did not  
632 influence the findings of the multiple regressions, we repeated the analysis excluding the 29  
633 species, which alleviated the skew and heteroscedasticity (Supplementary Fig. 2); the key finding  
634 of the multiple regression analysis, i.e., the interactive effect of MAT and MAP, was unaffected  
635 (Supplementary Table 8). Notably, the multiple regression analysis of leaf area versus growing  
636 season temperature and growing season precipitation also confirmed the trend, with greater  
637 normality and homoscedasticity of residuals, both when including all 1752 species and when  
638 excluding the 29 species with  $\text{MAT} < 0 \text{ }^\circ\text{C}$  (Supplementary Tables 7 and 8; Supplementary Figs.  
639 3-4).

640 We conducted hierarchical partitioning analyses on log transformed data to resolve the  
641 independent statistical associations of leaf size with individual climate variables<sup>142</sup>. Finally, we  
642 distinguished whether trait-climate correlations can be partially explained due to “triangular  
643 relationships”, i.e., when data are missing in one or more corners of the plot, an analysis that can  
644 provide special insights<sup>143,144</sup>. For example, a positive trait-climate correlation would arise at  
645 least in part from a triangular relationship if high trait values are few or absent at lower values of  
646 the climate variable, or if low trait values are few or absent at high values of the climate variable.  
647 To test for the presence of triangular relationships, we implemented quantile regression analyses,  
648 determining regression slopes fitted through the 5%, 50% and 95% quantiles of log transformed  
649 data<sup>145-147</sup>. A triangular relationship was supported when the regressions through the 95% and  
650 5% quantiles differed according to *t*-tests.

651

## 652 **Comparative analyses**

653 Comparative phylogenetic statistical analyses accounting for the effects of phylogenetic  
654 covariance on trait-climate and trait-trait relationships were conducted using the R Language and  
655 Environment version 3.4.1<sup>130</sup>.

656 Regression coefficients were estimated using phylogenetic least squares (PGLS) and/or  
657 phylogenetic reduced major axis (PRMA), in each case basing the phylogenetic correction on  
658 Pagel’s  $\lambda$ <sup>148,149</sup> estimated by maximum likelihood<sup>150</sup>. For PGLS, corPagel<sup>151</sup> was used in  
659 combination with gls<sup>150</sup> and optimized<sup>131</sup> to establish maximum likelihood estimates of  $\lambda$  in the 0  
660 – 1 range; for PRMA, phyl.RMA<sup>151</sup> was used. Confidence intervals for *b* estimated using PRMA  
661 were determined following ref<sup>152</sup>:

$$\pm \hat{b}(\sqrt{B+1} \pm \sqrt{B}), \text{ where } B = \frac{1-r^2}{N-2} f_{1-\alpha,1,N-2}$$

662 where  $\hat{b}$  is the fitted value for *b*; *r* is a correlation coefficient, for which we used a  
663 phylogenetically corrected estimate based on the variance-covariance matrix output by  
664 phyl.RMA; *N* is the number of pairs of observations; and  $f_{1-\alpha,1,N-2}$  is the critical value from the  
665 F distribution.

666 Differences in species-level trait means between C<sub>3</sub> and C<sub>4</sub> species were tested using a  
667 phylogenetically corrected ANOVA, both parametric (based on phylogenetic generalized least  
668 squares analysis, PGLS) and nonparametric<sup>153</sup>; *phyloANOVA* in R package<sup>151</sup>.

669 The impact of phylogenetic corrections was evaluated by comparing PGLS or PRMA  
670 with Pagel's  $\lambda$  estimated by maximum likelihood, to equivalent models in which Pagel's  $\lambda$  was  
671 set to 0. When using Pagel's  $\lambda$ , to assess normality and homoscedasticity assumptions we first  
672 extracted phylogenetic residuals. For PGLS, the function *residuals* was used to extract  
673 normalized residuals; for PRMA, a custom code (available on request), derived from an original  
674 provided by Professor Robert P. Freckleton, was used to produce an equivalent transformation of  
675 raw residuals obtained from *phyl.RMA*. Normality was tested using Anderson Darling tests<sup>154</sup>  
676 and heteroscedasticity using Bartlett's test<sup>130</sup>. Additionally, PGLS was used to estimate Pagel's  $\lambda$   
677 for phylogenetic residuals, which should be 0.

678 The PGLS and PRMA approaches used to test for scaling relationships of vein traits with  
679 leaf dimensions and to estimate the slopes of linearized power law relationships are phylogenetic  
680 approaches equivalent to ordinary least squares and reduced major axis regressions, respectively.  
681 Which of the two was used depended on the specific relationship tested. The least squares  
682 approach is preferable in cases when a dependent Y variable is related to an independent X  
683 variable, specifically when (1) there is much less error (i.e., natural variation and/or  
684 measurement error) in X than Y, and/or when (2) conceptually, Y is causally determined by, or  
685 to be predicted from, X, but never X from Y<sup>155,156</sup>. By contrast, the reduced major axis approach  
686 is preferable in cases when (1) X and Y have similar error, and/or when (2) X or Y are co-  
687 determined, or their relationship arises from an underlying functional coordination, or either  
688 could reasonably be predicted using the other; this approach is typically used in studies of  
689 allometric scaling relationships among functional traits or organ dimensions<sup>155,156</sup>. An exception  
690 to the use of reduced major axis for allometry is when testing whether the allometric slope of a  
691 relationship is consistent with an expected slope that was derived algebraically from other  
692 equations, as only least-squares slopes are robust to algebraic manipulation<sup>156</sup>. For example,  
693 PGLS would be selected over PRMA to test an expectation for the scaling slope of vein surface  
694 area per leaf area (VSA) with leaf length, that was derived algebraically by multiplying the  
695 expected scaling slopes of vein length per area (VLA) and vein diameter (VD) with leaf length,  
696 given that VSA is determined from VLA and VD (see, "*Quantification of leaf dimensions and*  
697 *vein traits*", above). Further, while least squares is appropriate for testing relationships of a  
698 dependent versus an independent trait, reduced major axis can be preferable for illustrating the

699 relationship in a plot, given that it captures more closely the central trend among two variables  
700 with high and/or similar error<sup>155,156</sup>.

701 Thus, we selected PGLS or PRMA for the tested relationships according to which was  
702 most appropriate given the above principles, while noting that the application of any single  
703 approach globally would not affect the findings of the study, but would reduce the accuracy of  
704 the specific slope estimates. We used PRMA to test relationships of traits with climate variables,  
705 as the magnitude of variation in modelled climate variables globally was similar to that for  
706 species means for leaf traits. We also used PRMA for testing scaling relationships of vein  
707 diameters with leaf length and width, and of xylem conduit diameters with vein diameters, given  
708 the preference of this approach for testing allometric relationships, and the similar error in the X  
709 and Y variables. We used PGLS for testing relationships of vein lengths, surface areas and  
710 volumes per leaf area with leaf dimensions, given the higher variability in the vein traits than leaf  
711 dimensions arising due to their determination from one or more vein traits as well as leaf  
712 dimensions (e.g., vein length per leaf area = vein number / leaf width). Further, PGLS was most  
713 appropriate for testing allometric slopes for the relationships of vein traits to leaf area, because  
714 the expectations for these slopes from the developmental model were derived algebraically from  
715 expected slopes of vein traits in relation to leaf length and leaf width<sup>155</sup>. Finally, we used PRMA  
716 in all figure plots to most clearly illustrate the central trends accounting for phylogeny<sup>155,156</sup>.

717 Lastly, we evaluated whether the scaling of vein traits with leaf dimensions differed  
718 between C<sub>3</sub> and C<sub>4</sub> species. C<sub>3</sub> and C<sub>4</sub> species were considered to differ significantly in trait-trait  
719 or trait-climate associations if significant relationships were found independently for both  
720 groups, and if there was no overlap in scaling slope 95% confidence intervals (CIs) using the  
721 selected regression approach (PGLS or PRMA).

722

### 723 **Modelling the impacts of leaf energy budget and testing hypotheses for the benefits of** 724 **smaller leaves under different climates**

725 We considered three hypotheses for the advantage of small leaf sizes in cold or dry climates  
726 based on their thinner boundary layer. Smaller leaves have been hypothesized to (1) experience  
727 less damage under extreme temperatures, i.e. chilling on colds nights and overheating on hot  
728 days<sup>3,157,158</sup>, (2) maintain higher rates of photosynthesis and/or higher leaf water use efficiency in  
729 cold and/or dry conditions<sup>19,20</sup> and (3) achieve higher gas exchange in favorable, warm and wet

730 climates<sup>4</sup>, which would provide an advantage in mitigating the shorter diurnal and/or seasonal  
731 growing periods of cold or dry climates.

732 To test hypothesis (1), i.e., that small grass leaves are typical in cold or dry climates  
733 globally because they avoid extreme temperatures, we calculated the minimum threshold of leaf  
734 size for chilling or overheating. We used the 100 cm<sup>2</sup> leaf size threshold for damage by nighttime  
735 chilling and 30 cm<sup>2</sup> for damage by daytime overheating, i.e., the lowest thresholds that were  
736 modelled for eudicotyledons globally given in Fig. 3 of ref. 3. Those leaf size thresholds for  
737 eudicotyledons were derived from estimated damage thresholds based on the “characteristic  
738 dimension” of the leaf ( $d$ , i.e., the diameter of the largest circle that can be delimited within a  
739 leaf) of 8.16 cm and 4.47 cm, according to eqn 4 in the supplemental information of ref 3 ( $LA =$   
740  $1.5 d^2$ ). Thus, we used these threshold values to exclude species with leaf width  $< 8.16$  cm and  $<$   
741  $4.47$  cm, and then tested whether the observed trends of leaf dimensions with MAT and MAP  
742 globally remained. Significant trends for this restricted species set would indicate that thresholds  
743 for leaf damage under extreme temperatures cannot explain trends for grasses with leaves  
744 smaller than those thresholds. By testing trends against these very low thresholds, we provided a  
745 very conservative test to establish that avoidance of extreme temperatures would not explain the  
746 global climatic distribution of grass leaf size.

747 To test hypotheses (2) and (3), we used heuristic leaf energy balance modelling to  
748 simulate the consequences for gas exchange of leaf sizes varying in size<sup>159</sup>. Using the Tealeaves  
749 R package<sup>159</sup>, given inputs of leaf width, wind speed, stomatal conductance and air temperature,  
750 we simulated boundary layer conductance, leaf temperature, and transpiration rate. To represent  
751 the bulk of the global range of grass leaf size, we focused on comparing the global 5<sup>th</sup> and 95<sup>th</sup>  
752 quantiles of leaf width (0.1 cm and 2.7 cm). We simulated leaves in wet and dry conditions by  
753 setting stomatal conductance values at 0.4 mol m<sup>-2</sup> s<sup>-1</sup> and 0.2 mol m<sup>-2</sup> s<sup>-1</sup>, respectively<sup>160</sup>; our  
754 tests showed that selecting other values would yield similar qualitative results. To represent  
755 warm and cold climates we simulated gas exchange under air temperatures of 315 K and 280 K  
756 (41.85 °C and 6.85 °C respectively)<sup>161</sup>. All other physical and environmental inputs were  
757 maintained constant at typical values<sup>159</sup>. We used the output values of leaf temperature and  
758 boundary layer conductance to simulate C<sub>3</sub> photosynthetic rate for leaves of different widths  
759 using the Farquhar model<sup>162,163</sup>. We tested these effects at the two wind speeds, 0.1 m/s and 2  
760 m/s. Lastly, we tested simulations for both amphistomatous and hypostomatous leaves, and we

761 present results for amphistomatous leaves given that most grasses are amphistomatous<sup>164</sup>. To test  
762 for the potential benefit of smaller leaves, we calculated the ratios of photosynthetic rate,  
763 transpiration and leaf water use efficiency for a small relative to large leaf; values > 1 indicate an  
764 advantage for the small leaf in cold or dry conditions. To test for the potential benefit of smaller  
765 leaves in mitigating a shorter period with favourable climate, we calculated the ratios of  
766 photosynthetic rate, transpiration and leaf water use efficiency under warm and wet conditions  
767 for a small versus a large leaf; again, values > 1 signify a small leaf advantage.

768

### 769 **Supplementary References**

770

771 48 Kluyver, T. A. & Osborne, C. P. Taxonome: a software package for linking biological  
772 species data. *Ecol. Evol.* **3**, 1262-1265 (2013).

773 49 Cayuela, L., Granzow-de la Cerda, I., Albuquerque, F. S. & Golicher, D. J.  
774 TAXONSTAND: An R package for species names standardisation in vegetation  
775 databases. *Methods Ecol. Evol.* **3**, 1078-1083 (2012).

776 50 Fick, S. E. & Hijmans, R. J. WorldClim 2: new 1-km spatial resolution climate surfaces  
777 for global land areas. *Int J. Climatol.* **37**, 4302-4315 (2017).

778 51 Cherlet, M. H., C.; Reynolds, J.; Hill, J.; Sommer, S.; von Maltitz, G. *World Atlas of*  
779 *Desertification*. 3rd edn, (Publication Office of the European Union, 2018).

780 52 Harris, I., Jones, P. D., Osborn, T. J. & Lister, D. H. Updated high-resolution grids of  
781 monthly climatic observations - the CRU TS3.10 Dataset. *Int. J. Climatol.* **34**, 623-642  
782 (2014).

783 53 Lasky, J. R. et al. Characterizing genomic variation of *Arabidopsis thaliana*: the roles of  
784 geography and climate. *Mol. Ecol.* **21**, 5512-5529 (2012).

785 54 Sexton, J. P., McIntyre, P. J., Angert, A. L. & Rice, K. J. Evolution and Ecology of  
786 Species Range Limits. *Ann. Rev. Ecol. Evol. & Syst.* **40**, 415-436 (2009).

787 55 Dengler, N. G., Dengler, R. E. & Hattersley, P. W. Differing ontogenetic origins of PCR  
788 (Kranz) sheaths in leaf blades of C<sub>4</sub> grasses (*Poaceae*). *Am. J. Bot.* **72**, 284-302 (1985).

789 56 Dengler, N. G., Woodvine, M. A., Donnelly, P. M. & Dengler, R. E. Formation of  
790 vascular pattern in developing leaves of the C<sub>4</sub> grass *Arundinella hirta*. *Int. J. Plant Sci.*  
791 **158**, 1-12 (1997).

- 792 57 Ikenberry, G.-J. J. *Developmental vegetative morphology of avena sativa* PhD thesis,  
793 Iowa State University, (1959).
- 794 58 Kaufman, P. B. & Brock, T. G. Structural development of the oat plant. *Agronomy*  
795 *Monograph* **33**, 53 - 75 (1992).
- 796 59 Hitch, P. A. & Sharman, B. C. Initiation of procambial strands in leaf primordia of  
797 *Dactylis glomerata* L as an example of a temperate herbage grass. *Ann. Bot-London* **32**,  
798 153-164 (1968).
- 799 60 Davidson, J. L. & Milthorpe, F. L. Leaf growth in *Dactylis glomerata* following  
800 defoliation. *Ann. Bot-London* **30**, 173-184 (1966).
- 801 61 Volenec, J. J. & Nelson, C. J. Cell dynamics in leaf meristems of contrasting tall fescue  
802 genotypes. *Crop Sci* **21**, 381-385 (1981).
- 803 62 Macadam, J. W. & Nelson, C. J. Specific leaf weight in zones of cell division, elongation  
804 and maturation in tall fescue leaf blades. *Ann. Bot-London* **59**, 369-376 (1987).
- 805 63 Macadam, J. W., Volenec, J. J. & Nelson, C. J. Effects of nitrogen on mesophyll cell  
806 division and epidermal cell elongation in tall fescue leaf blades. *Plant Physiol.* **89**, 549-  
807 556 (1989).
- 808 64 Skinner, R. H. & Nelson, C. J. Elongation of the grass leaf and its relationship to the  
809 phyllochron. *Crop Sci.* **35**, 4-10 (1995).
- 810 65 Skinner, R. H. & Nelson, C. J. Epidermal cell division and the coordination of leaf and  
811 tiller development. *Ann. Bot-London* **74**, 9-15 (1994).
- 812 66 Maurice, I., Gastal, F. & Durand, J. L. Generation of form and associated mass deposition  
813 during leaf development in grasses: a kinematic approach for non-steady growth. *Ann.*  
814 *Bot-London* **80**, 673-683 (1997).
- 815 67 Durand, J. L., Schaufele, R. & Gastal, F. Grass leaf elongation rate as a function of  
816 developmental stage and temperature: Morphological analysis and modelling. *Ann. Bot-*  
817 *London* **83**, 577-588 (1999).
- 818 68 Martre, P., Durand, J. L. & Cochard, H. Changes in axial hydraulic conductivity along  
819 elongating leaf blades in relation to xylem maturation in tall fescue. *New Phytol.* **146**,  
820 235-247 (2000).

821 69 Martre, P. & Durand, J. L. Quantitative analysis of vasculature in the leaves of *Festuca*  
822 *arundinacea* (*Poaceae*): Implications for axial water transport. *Int. J. Plant Sci.* **162**, 755-  
823 766 (2001).

824 70 Gallagher, J. N. Field studies of cereal leaf growth 1. Initiation and expansion in relation  
825 to temperature and ontogeny. *J Exp Bot* **30**, 625-636 (1979).

826 71 Gallagher, J. N. & Biscoe, P. V. Field studies of cereal leaf growth 3. Barley leaf  
827 extension in relation to temperature, irradiance, and water potential. *J. Exp. Bot.* **30**, 645-  
828 655 (1979).

829 72 Dannenhoffer, J. M., Ebert, W. & Evert, R. F. Leaf vasculature in barley, *Hordeum*  
830 *vulgare* (*Poaceae*). *Am. J. Bot.* **77**, 636-652 (1990).

831 73 Dannenhoffer, J. M. & Evert, R. F. Development of the vascular system in the leaf of  
832 barley (*Hordeum vulgare* L.). *Int. J. Plant Sci.* **155**, 143-157 (1994).

833 74 Trivett, C. L. & Evert, R. F. Ontogeny of the vascular bundles and contiguous tissues in  
834 the barley leaf blade. *Int. J. Plant Sci.* **159**, 716-732 (1998).

835 75 Soper, K. & Mitchell, K. J. The developmental anatomy of perennial ryegrass (*Lolium*  
836 *perenne* L.). *NZ J. Sci. Tech.* **37**, 484-504 (1956).

837 76 Schnyder, H., Nelson, C. J. & Coutts, J. H. Assessment of spatial distribution of growth  
838 in the elongation zone of grass leaf blades. *Plant Physiol.* **85**, 290-293 (1987).

839 77 Arredondo, J. T. & Schnyder, H. Components of leaf elongation rate and their  
840 relationship to specific leaf area in contrasting grasses. *New Phytol.* **158**, 305-314 (2003).

841 78 Kaufman, P. B. Development of the shoot of *Oryza sativa* L. - II. Leaf histogenesis.  
842 *Phytomorphology* **9**, 277-311 (1959).

843 79 Yamazaki, K. Studies on the leaf formation in rice plants: I. Observation on the  
844 successive development of the leaf. *Jap. J. Crop Sci.* **31**, 371-378 (1963).

845 80 Chonan, N. K., H.; Matsuda, T. Morphology on vascular bundles of leaves in gramineous  
846 crops: I. Observations on vascular bundles of leaf blades, sheaths and internodes in  
847 riceplants. *Jap. J. Crop Sci.* **43**, 425-432 (1974).

848 81 Hoshikawa, K. *The growing rice plant: an anatomical monograph.* (Nobunkyo, 1989).

849 82 Matsukura, C. et al. Transverse vein differentiation associated with gas space formation -  
850 Fate of the middle cell layer in leaf sheath development of rice. *Ann. Bot-London* **85**, 19-  
851 27 (2000).



- 852 83 Itoh, J. et al. Rice plant development: from zygote to spikelet. *Plant Cell Physiol.* **46**, 23-  
853 47 (2005).
- 854 84 Sakaguchi, J. & Fukuda, H. Cell differentiation in the longitudinal veins and formation of  
855 commissural veins in rice (*Oryza sativa*) and maize (*Zea mays*). *J. Plant Res.* **121**, 593-  
856 602 (2008).
- 857 85 Parent, B., Conejero, G. & Tardieu, F. Spatial and temporal analysis of non-steady  
858 elongation of rice leaves. *Plant Cell Environ.* **32**, 1561-1572 (2009).
- 859 86 Begg, J. E. & Wright, M. J. Growth and development of leaves from intercalary  
860 meristems in *Phalaris arundinacea* L. *Nature* **194**, 1097-1098 (1962).
- 861 87 Colbert, J. T. & Evert, R. F. Leaf vasculature in sugarcane (*Saccharum officinarum* L).  
862 *Planta* **156**, 136-151 (1982).
- 863 88 Bernstein, N., Silk, W. K. & Lauchli, A. Growth and development of sorghum leaves  
864 under conditions of NaCl stress - Spatial and temporal aspects of leaf growth inhibition.  
865 *Planta* **191**, 433-439 (1993).
- 866 89 Sud, R. M. & Dengler, N. G. Cell lineage of vein formation in variegated leaves of the C<sub>4</sub>  
867 grass *Stenotaphrum secundatum*. *Ann. Bot-London* **86**, 99-112 (2000).
- 868 90 Sharman, B. C. & Hitch, P. A. Initiation of procambial strands in leaf primordia of bread  
869 wheat *Triticum aestivum* L. *Ann. Bot-London* **31**, 229-243 (1967).
- 870 91 Blackman, E. The morphology and development of cross veins in the leaves of bread  
871 wheat (*Triticum aestivum* L.). *Ann. Bot-London* **35**, 653-665 (1971).
- 872 92 Kemp, D. R. The location and size of the extension zone of emerging wheat leaves. *New*  
873 *Phytol.* **84**, 729-737 (1980).
- 874 93 Paolillo, D. J. Protoxylem maturation in the seedling leaf of wheat. *Am. J. Bot.* **82**, 337-  
875 345 (1995).
- 876 94 Beemster, G. T. S. & Masle, J. The role of apical development around the time of leaf  
877 initiation in determining leaf width at maturity in wheat seedlings (*Triticum aestivum* L.)  
878 with impeded roots. *J. Exp. Bot.* **47**, 1679-1688 (1996).
- 879 95 Sharman, B. C. Developmental anatomy of the shoot of *Zea mays* L. *Ann. Bot-London* **6**,  
880 245-282 (1942).
- 881 96 Esau, K. Ontogeny of the vascular bundle in *Zea mays*. *Hilgardia* **15**, 327-368 (1943).

- 882 97 Bosabalidis, A. M., Evert, R. F. & Russin, W. A. Ontogeny of the vascular bundles and  
883 contiguous tissues in the maize leaf blade. *Am. J. Bot.* **81**, 745-752 (1994).
- 884 98 Poethig, S. in *Contemporary problems in plant anatomy* (ed R. A.; Dickison White, W.  
885 C.) (Academic Press, 1984).
- 886 99 Russell, S. H. & Evert, R. F. Leaf Vasculature in *Zea mays*-L. *Planta* **164**, 448-458  
887 (1985).
- 888 100 Smith, L. G., Greene, B., Veit, B. & Hake, S. A dominant mutation in the maize  
889 homeobox gene, knotted-1, causes its ectopic expression in leaf-cells with altered fates.  
890 *Development* **116**, 21-& (1992).
- 891 101 Fournier, C. & Andrieu, B. A 3D architectural and process-based model of maize  
892 development. *Ann. Bot-London* **81**, 233-250 (1998).
- 893 102 Muller, B., Reymond, M. & Tardieu, F. The elongation rate at the base of a maize leaf  
894 shows an invariant pattern during both the steady-state elongation and the establishment  
895 of the elongation zone. *J. Exp. Bot.* **52**, 1259-1268 (2001).
- 896 103 Muller, B. et al. Association of specific expansins with growth in Maize leaves is  
897 maintained under environmental, genetic, and developmental sources of variation. *Plant*  
898 *Physiol.* **143**, 278-290 (2007).
- 899 104 Johnston, R., Leiboff, S. & Scanlon, M. J. Ontogeny of the sheathing leaf base in maize  
900 (*Zea mays*). *New Phytol.* **205**, 306-315 (2015).
- 901 105 Benhajsalah, H. & Tardieu, F. Temperature affects expansion rate of maize leaves  
902 without change in spatial distribution of cell length - Analysis of the coordination  
903 between cell division and cell expansion. *Plant Physiol.* **109**, 861-870 (1995).
- 904 106 Tardieu, F., Reymond, M., Hamard, P., Granier, C. & Muller, B. Spatial distributions of  
905 expansion rate, cell division rate and cell size in maize leaves: a synthesis of the effects  
906 of soil water status, evaporative demand and temperature. *J. Exp. Bot.* **51**, 1505-1514  
907 (2000).
- 908 107 Runions, A. et al. Modeling and visualization of leaf venation patterns. *Acm T. Graphic*  
909 **24**, 702-711 (2005).
- 910 108 Scarpella, E. & Meijer, A. H. Pattern formation in the vascular system of monocot and  
911 dicot plant species. *New Phytol.* **164**, 209-242 (2004).

- 912 109 Baskin, T. I. Anisotropic expansion of the plant cell wall. *Ann. Rev. Cell. Dev.* **21**, 203-  
913 222 (2005).
- 914 110 Fujita, H. & Mochizuki, A. The origin of the diversity of leaf venation pattern. *Dev. Dyn.*  
915 **235**, 2710-272 (2006).
- 916 111 Granier, C. & Tardieu, F. Multi-scale phenotyping of leaf expansion in response to  
917 environmental changes: the whole is more than the sum of parts. *Plant Cell Environ.* **32**,  
918 1175-1184 (2009).
- 919 112 Scarpella, E., Barkoulas, M. & Tsiantis, M. Control of leaf and vein development by  
920 auxin. *Csh Perspect Biol* **2** (2010).
- 921 113 Gazquez, A. & Beemster, G. T. S. What determines organ size differences between  
922 species? A meta-analysis of the cellular basis. *New Phytol.* **215**, 299-308 (2017).
- 923 114 Scarpella, E. The logic of plant vascular patterning. Polarity, continuity and plasticity in  
924 the formation of the veins and of their networks. *Curr. Opin. Genet. Dev.* **45**, 34-43  
925 (2017).
- 926 115 Berlyn, G. P. M., J. P. *Botanical Microtechnique and Cytochemistry.* (Iowa State  
927 University Press, 1976).
- 928 116 Kemp, C. D. Methods of estimating leaf area of grasses from linear measurements. *New.*  
929 *Phytol.* **24**, 491-299 (1960).
- 930 117 Stickler, F. C., Wearden, S. & Pauli, A. W. Leaf area determination in grain sorghum.  
931 *Agronomy* **53**, 187-188 (1961).
- 932 118 Shi, P. et al. Leaf area-length allometry and its implications in leaf shape evolution.  
933 *Trees* **33**, 1073-1085 (2019).
- 934 119 Ellis, R. P. A procedure for standardizing comparative leaf anatomy in the *Poaceae*. I.  
935 The leaf blade as viewed in transverse section. *Bothalia* **12**, 65-109 (1976).
- 936 120 Evert, R. F. *Esau's plant anatomy: meristems, cells, and tissues of the plant body: their*  
937 *structure, function, and development.* (John Wiley & Sons, 2006).
- 938 121 Neufeld, H. S. et al. Genotypic variability in vulnerability of leaf xylem to cavitation in  
939 water-stressed and well-irrigated sugarcane. *Plant Physiol.* **100**, 1020-1028 (1992).
- 940 122 Tyree, M. T., Zimmermann, M. H. & Zimmermann, M. H. *Xylem structure and the*  
941 *ascent of sap.* 2nd edn, (Springer, 2002).
- 942 123 Wright, I. J. et al. The world-wide leaf economics spectrum. *Nature* **428**, 821-827 (2004).

943 124 Aliscioni, S. et al. New grass phylogeny resolves deep evolutionary relationships and  
944 discovers C<sub>4</sub> origins. *New Phytol.* **193**, 304-312 (2012).

945 125 Taylor, S. H. et al. Photosynthetic pathway and ecological adaptation explain stomatal  
946 trait diversity amongst grasses. *New Phytol.* **193**, 387-396 (2012).

947 126 Edgar, R. C. MUSCLE: multiple sequence alignment with high accuracy and high  
948 throughput. *Nucleic Acids Res* **32**, 1792-1797 (2004).

949 127 Drummond, A. J. & Rambaut, A. BEAST: Bayesian evolutionary analysis by sampling  
950 trees. *Bmc Evol Biol* **7** (2007).

951 128 Christin, P. A. et al. Molecular Dating, Evolutionary Rates, and the Age of the Grasses.  
952 *Syst Biol* **63**, 153-165 (2013).

953 129 Prasad, V. et al. Late Cretaceous origin of the rice tribe provides evidence for early  
954 diversification in Poaceae. *Nat. Commun.* **2** (2011).

955 130 R: A language and environment for statistical computing (R Foundation for Statistical  
956 Computing, Vienna, Austria, 2019).

957 131 Paradis, E. & Schliep, K. ape 5.0: an environment for modern phylogenetics and  
958 evolutionary analyses in R. *Bioinformatics* **35**, 526-528(2019).

959 132 Spriggs, E. L., Christin, P. A. & Edwards, E. J. (ed Dryad Digital Repository) (2014).

960 133 Felsenstein, J. Phylogenies and the comparative method. *Am. Nat.* **125**, 1-15 (1985).

961 134 Schmerler, S. B. et al. Evolution of leaf form correlates with tropical–temperate  
962 transitions in *Viburnum* (Adoxaceae). *P. Royal. Soc. B.* **279**, 3905-3913 (2012).

963 135 Fletcher, L. R. et al. Evolution of leaf structure and drought tolerance in species of  
964 Californian *Ceanothus*. *Am. J. Bot.* **105**, 1672-1687 (2018).

965 136 Bramer, I. et al. in *Next Generation Biomonitoring: Part I: Advances in Ecological*  
966 *Research* 101-161 (2018).

967 137 Zanne, A. E. et al. Three keys to the radiation of angiosperms into freezing environments.  
968 *Nature* **514**, 394-394 (2014).

969 138 Watcharamongkol, T., Christin, P. A. & Osborne, C. P. C<sub>4</sub> photosynthesis evolved in  
970 warm climates but promoted migration to cooler ones. *Ecol. Lett.* **21**, 376-383 (2018).

971 139 Burnham, K. P. & Anderson, D. R. *Model selection and multimodel inference*. 2 edn,  
972 (Springer, 2002).

973 140 Gelman, A. & Hill, J. *Data analysis using regression and multilevel/hierarchical models*.  
974 (Cambridge University Press, 2006).

975 141 Faraway, J. J. *Linear Models with R*. (Chapman & Hall/CRC, 2009).

976 142 Murray, K. & Conner, M. M. Methods to quantify variable importance: implications for  
977 the analysis of noisy ecological data. *Ecology* **90**, 348-355 (2009).

978 143 Westoby, M. & Wright, I. J. Land-plant ecology on the basis of functional traits. *Trends*  
979 *Ecol. Evol.* **21**, 261-268 (2006).

980 144 Grubb, P. J. Trade-offs in interspecific comparisons in plant ecology and how plants  
981 overcome proposed constraints. *Plant Ecol. Divers.* **9**, 3-33 (2016).

982 145 Cade, B. S. & Noon, B. R. A gentle introduction to quantile regression for ecologists.  
983 *Front. Ecol. Environ.* **1**, 412-420 (2003).

984 146 Grubb, P. J., Coomes, D. A. & Metcalfe, D. J. Comment on "A Brief History of Seed  
985 Size". *Science* **310**, 781-783 (2005).

986 147 Moles, A. T. *et al.* Global patterns in plant height. *J. Ecol.* **97**, 923-932 (2009).

987 148 Pagel, M. Inferring the historical patterns of biological evolution. *Nature* **401**, 877-884  
988 (1999).

989 149 Freckleton, R. P., Harvey, P. H. & Pagel, M. Phylogenetic analysis and comparative data:  
990 A test and review of evidence. *Am. Nat.* **160**, 712-726 (2002).

991 150 "nlme" (R package version 3.1-140) (2019).

992 151 Revell, L. J. phytools: an R package for phylogenetic comparative biology (and other  
993 things). *Methods Ecol. Evol.* **3**, 217-223 (2012).

994 152 Warton, D. I., Wright, I. J., Falster, D. S. & Westoby, M. Bivariate line-fitting methods  
995 for allometry. *Biol. Rev.* **81**, 259-291 (2006).

996 153 Garland, T., Dickerman, A. W., Janis, C. M. & Jones, J. A. Phylogenetic Analysis of  
997 Covariance by Computer-Simulation. *Syst. Biol.* **42**, 265-292 (1993).

998 154 "nortest: Tests for normality" (R package version 1.0-4) (2015).

999 155 Poorter, H. & Sack, L. Pitfalls and possibilities in the analysis of biomass allocation  
1000 patterns in plants. *Front. Plant Sci.* **3**, 1-10 (2012).

1001 156 Smith, R. J. Use and Misuse of the Reduced Major Axis for Line-Fitting. *Am. J. Phys.*  
1002 *Anthropol.* **140**, 476-486 (2009).

1003 157 Gates, D. M. Energy, Plants, and Ecology. *Ecology* **46**, 1-13 (1965).

1004 158 Lusk, C. H. et al. Frost and leaf-size gradients in forests: global patterns and experimental  
1005 evidence. *New Phytol.* **219**, 565-573 (2018).

1006 159 Muir, C. D. tealeaves: an R package for modelling leaf temperature using energy budgets.  
1007 *Aob Plants* **11**, 1-10 (2019).

1008 160 Taylor, S. H. et al. Ecophysiological traits in C<sub>3</sub> and C<sub>4</sub> grasses: a phylogenetically  
1009 controlled screening experiment. *New Phytol.* **185**, 780-791 (2010).

1010 161 Huang, M. et al. Air temperature optima of vegetation productivity across global biomes.  
1011 *Nat. Ecol. Evol.* **3**, 772-779 (2019).

1012 162 Farquhar, G. D., Caemmerer, S. V. & Berry, J. A. A biochemical model of photosynthetic  
1013 CO<sub>2</sub> assimilation in leaves of C<sub>3</sub> species. *Planta* **149**, 78-90 (1980).

1014 163 Bernacchi, C. J., Pimentel, C. & Long, S. P. In vivo temperature response functions of  
1015 parameters required to model RuBP-limited photosynthesis. *Plant Cell Environ.* **26**,  
1016 1419-1430 (2003).

1017 164 Muir, C. D. Making pore choices: repeated regime shifts in stomatal ratio. *P. Royal. Soc.*  
1018 *B.* **282**, 1-9 (2012).

1019 165 Brummitt, R. K. World geographical scheme for recording plant distributions. (2001).

1020 166 Redmann, R. E. Adaptation of grasses to water-stress - leaf rolling and stomate  
1021 distribution. *Ann. Mo. Bot. Gard.* **72**, 833-842 (1985).

1022 167 Forrestel, E. J. et al. Different clades and traits yield similar grassland functional  
1023 responses. *P. Natl. Acad. Sci. USA* **114**, 705-710 (2017).

1024 168 Liu, H., Edwards, E. J., Freckleton, R. P. & Osborne, C. P. Phylogenetic niche  
1025 conservatism in C<sub>4</sub> grasses. *Oecologia* **170**, 835-845 (2012).

1026 169 Liu, H. & Osborne, C. P. Water relations traits of C<sub>4</sub> grasses depend on phylogenetic  
1027 lineage, photosynthetic pathway, and habitat water availability. *J. Exp. Bot.* **66**, 761-773  
1028 (2015).

1029 170 Jardine, E. C., Thomas, G. H., Forrestel, E. J., Lehmann, C. E. R. & Osborne, C. P. The  
1030 global distribution of grass functional traits within grassy biomes. *J. Biogeogr.* **47**, 553-  
1031 565 (2020).

1032 171 Kawai, K. & Okada, N. Leaf vascular architecture in temperate dicotyledons: correlations  
1033 and link to functional traits. *Planta* **251**, 1-12 (2019).

- 1034 172 Medeiros, C. D. et al. An extensive suite of functional traits distinguishes Hawaiian wet  
1035 and dry forests and enables prediction of species vital rates. *Funct. Ecol.* **33**, 712-734  
1036 (2019).
- 1037 173 Li, F. L. et al. Linking leaf hydraulic properties, photosynthetic rates, and leaf lifespan in  
1038 xerophytic species: a test of global hypotheses. *Am. J. Bot.* **105**, 1858-1868 (2018).
- 1039 174 Blackman, C. J. et al. The links between leaf hydraulic vulnerability to drought and key  
1040 aspects of leaf venation and xylem anatomy among 26 Australian woody angiosperms  
1041 from contrasting climates. *Ann. Bot-London* **122**, 59-67 (2018).
- 1042 175 Gleason, S. M. et al. Vessel scaling in evergreen angiosperm leaves conforms with  
1043 Murray's law and area-filling assumptions: implications for plant size, leaf size and cold  
1044 tolerance. *New Phytol.* **218**, 1360-1370 (2018).
- 1045 176 Savi, T. et al. Morpho-anatomical and physiological traits in saplings of drought-tolerant  
1046 Mediterranean woody species. *Trees-Struct. Funct.* **31**, 1137-1148 (2017).
- 1047 177 Brodribb, T. J., Bienaime, D. & Marmottant, P. Revealing catastrophic failure of leaf  
1048 networks under stress. *P. Natl. Acad. Sci. USA* **113**, 4865-4869 (2016).
- 1049 178 Schneider, J. V. et al. Water supply and demand remain coordinated during breakdown of  
1050 the global scaling relationship between leaf size and major vein density. *New Phytol.*  
1051 **214**, 473-486 (2017).
- 1052 179 Coomes, D. A., Heathcote, S., Godfrey, E. R., Shepherd, J. J. & Sack, L. Scaling of  
1053 xylem vessels and veins within the leaves of oak species. *Biol. Letters* **4**, 302-306 (2008).
- 1054 180 Yao, G. Q. et al. Combined high leaf hydraulic safety and efficiency provides drought  
1055 tolerance in *Caragana* species adapted to low mean annual precipitation. *New Phytol.*  
1056 (2020).
- 1057 181 McKown, A. D., Akamine, M. E. & Sack, L. Trait convergence and diversification  
1058 arising from a complex evolutionary history in Hawaiian species of *Scaevola*. *Oecologia*  
1059 **181**, 1083-1100 (2016).
- 1060 182 Kawai, K. & Okada, N. How are leaf mechanical properties and water-use traits  
1061 coordinated by vein traits? A case study in Fagaceae. *Funct. Ecol.* **30**, 527-536 (2016).
- 1062 183 Dunbar-Co, S., Sporck, Margaret J. & Sack, L. Leaf Trait diversification and design in  
1063 seven rare taxa of the hawaiian plantago radiation. *Int. J. Plant Sci.* **170**, 61-75 (2009).

1064 184 Scoffoni, C. et al. Light-induced plasticity in leaf hydraulics, venation, anatomy, and gas  
1065 exchange in ecologically diverse Hawaiian lobeliads. *New Phytol.* **207**, 43-58 (2015).

1066 185 Lu, Z. et al. Potassium mediates coordination of leaf photosynthesis and hydraulic  
1067 conductance by modifications of leaf anatomy. *Plant Cell Environ.* **42**, 2231-2244  
1068 (2019).

1069 186 Nardini, A., Peda, G. & La Rocca, N. Trade-offs between leaf hydraulic capacity and  
1070 drought vulnerability: morpho-anatomical bases, carbon costs and ecological  
1071 consequences. *New Phytol.* **196**, 788-798 (2012).

1072 187 Brocious, C. A. & Hacke, U. G. Stomatal conductance scales with petiole xylem traits in  
1073 *Populus* genotypes. *Funct. Plant Biol.* **43**, 553-562 (2016).

1074 188 Mauri, R. et al. Leaf hydraulic properties are decoupled from leaf area across coffee  
1075 species. *Trees* **34**, 1507-1514 (2020).

1076 189 Nardini, A., Ounapuu-Pikas, E. & Savi, T. When smaller is better: leaf hydraulic  
1077 conductance and drought vulnerability correlate to leaf size and venation density across  
1078 four *Coffea arabica* genotypes. *Funct. Plant Biol.* **41**, 972-982 (2014).

1079 190 Mediavilla, S., Martín, I. & Escudero, A. Vein and stomatal traits in leaves of three co-  
1080 occurring *Quercus* species differing in leaf life span. *Eur. J. For. Res.* **139**, 829-840  
1081 (2020).

1082 191 Wang, J.-H., Cai, Y.-F., Li, S.-F. & Zhang, S.-B. Photosynthetic acclimation of  
1083 rhododendrons to light intensity in relation to leaf water-related traits. *Plant Ecol.* **221**,  
1084 407-420 (2020).

1085 192 Cardoso, A. A. et al. Extended differentiation of veins and stomata is essential for the  
1086 expansion of large leaves in *Rheum rhabarbarum*. *Am. J. Bot.* **105**, 1967-1974 (2018).

1087 193 Taneda, H. & Terashima, I. Co-ordinated development of the leaf midrib xylem with the  
1088 lamina in *Nicotiana tabacum*. *Ann. Bot.* **110**, 35-45 (2012).

1089 194 Sevanto, S., Holbrook, N. M. & Ball, M. C. Freeze/Thaw-Induced embolism: probability  
1090 of critical bubble formation depends on speed of ice formation. *Front. Plant Sci.* **3**, 1-12  
1091 (2012).

1092 195 McKown, A. D., Cochard, H. & Sack, L. Decoding leaf hydraulics with a spatially  
1093 explicit model: Principles of venation architecture and implications for its evolution. *Am.*  
1094 *Nat.* **175**, 447-460 (2010).



1095 196 Spriggs EL, Christin P-A, Edwards EJ (2014) C<sub>4</sub> Photosynthesis promoted species  
1096 diversification during the miocene grassland expansion. *PloS One* **9**, 1-10 (2014).

1097

### 1098 **Acknowledgments**

1099 We thank T Cheng, W Deng, A.C. Diener, A Kooner, M McMaster, C Muir, S Moshrefi, A. J.  
1100 Patel, A Sayari and M. S. Vorontsova for logistical assistance. **Funding:** Funding was provided  
1101 by the U.S. National Science Foundation (grants 1457279, 1951244 and 2017949), the Natural  
1102 Environment Research Council (grants NE/DO13062/1 and NE/T000759/1) and a Royal Society  
1103 University Research Fellowship (grant URF\R\180022).

1104

### 1105 **Author contributions**

1106 *Conceptualization:* ASB, SHT, CPO, LS; *Data curation & Writing – review & editing:* ASB,  
1107 SHT, JPK, CV, YZ, TW, CS, EJE, PAC, CPO, LS; *Formal analysis:* ASB, SHT, JPK, CV, YZ,  
1108 TW, CS, PAC, LS; *Funding acquisition:* CPO, LS; *Investigation:* ASB, SHT, JPK, TW, CS,  
1109 EJE, PAC, CPO, LS; *Methodology:* ASB, SHT, JPK, TW, CS, EJE, PAC, CPO, LS; *Project*  
1110 *administration:* ASB, SHT, JPK, CPO, LS *Resources:* ASB, SHT, JPK, TW, CS, EJE, PAC,  
1111 CPO, LS; *Software:* ASB, SHT, TW, PAC; *Supervision:* ASB, SHT, JPK, CPO, LS; *Validation:*  
1112 ASB, SHT, CPO, LS; *Visualization:* ASB, SHT, TW, CV, PAC; *Writing – original draft:* ASB,  
1113 SHT, LS

1114

### 1115 **Competing interests**

1116 We declare no competing interests. All data are available in the main text or supplementary  
1117 materials.

1118

### 1119 **Additional information**

1120 Supplementary information is available online. Reprints and permissions information is available  
1121 online at [www.nature.com/reprints](http://www.nature.com/reprints). Correspondence and requests for materials should be  
1122 addressed to A.S.B.

1123

1124

1125

1126 **Data availability**

1127 Data utilized in this study are provided in the supplementary materials. Leaf trait data for the  
1128 1752 grass species was provided by the published Kew Grassbase Database  
1129 (<http://www.kew.org/data/grassbase/>). Species' climate data were extracted from WorldClim 2 5-  
1130 arc minute resolution (<https://worldclim.org/version2>) and from CRU TS4.01 01  
1131 ([https://crudata.uea.ac.uk/cru/data/hrg/cru\\_ts\\_4.01/](https://crudata.uea.ac.uk/cru/data/hrg/cru_ts_4.01/)) based on each species' geographical records  
1132 (<http://www.gbif.org>). Photosynthetic trait data and field locations were extracted for the 13 C<sub>3</sub>  
1133 grass species for which this was available in GLOPNET  
1134 (<http://bio.mq.edu.au/~iwright/glopian.htm>).

1135

1136 **Code availability**

1137 Custom-written R code is available on GitHub (<https://github.com/smuell-tylor/grass-leaf-size->).

1138

1139 **Extended Data Figure Legends**

1140

1141 **Extended Data Fig. 1 Time-calibrated phylogenetic trees for 1752 worldwide grass species**  
1142 **and for 27 grass species grown in a greenhouse common garden. (a)** phylogeny for 1752  
1143 species trimmed from that of reference 196 and used for analyses of global scaling of leaf size  
1144 with climate. C<sub>3</sub> and C<sub>4</sub> species in black and red respectively ( $n = 840$  and  $n = 912$  respectively).  
1145 **(b)** phylogeny for 27 species used for analyses of leaf vein scaling (black branches = 11 C<sub>3</sub>, red  
1146 branches = 16 C<sub>4</sub>), emphasizing the inclusion of 11 independent C<sub>4</sub> origins. World map with  
1147 distributions of **(c)** 11 C<sub>3</sub> species and, **(d)** 16 C<sub>4</sub> species.

1148

1149 **Extended Data Fig. 2. Worldwide relationships of grass leaf and plant dimensions with**  
1150 **species' native climate, the global distribution of grass leaf size, and the scaling of grass leaf**  
1151 **and plant dimensions. Relationships of (a) – (c) Leaf length, (d) – (f) leaf width, (g) – (i) leaf**  
1152 **area, and (j) – (l) culm height with mean annual temperature (MAT, °C), mean annual**  
1153 **precipitation (MAP, mm) and aridity index (AI). (m-o) Average across species of leaf area for**  
1154 **each country in the global database (International Working Group on Taxonomic Databases for**  
1155 **Plant Sciences, TDWG level 3 spatial units<sup>168</sup>), including countries for which > 20 species occur**  
1156 **in the global database (21 – 547 species for each country; gray for countries with < 20 species**

1157 represented), i.e., **(m)** mean leaf area **(n)** median leaf area and **(o)** leaf area for the largest leafed  
 1158 species **(p)** The scaling of leaf area with leaf length and **(q)** leaf width, **(r)** leaf area with culm  
 1159 height, **(s)** culm height with leaf length and **(t)** leaf width and **(u)** leaf width with leaf length.  
 1160 Leaf trait and climate data provided in Supplementary Table 2.  $N = 1752$  globally distributed  
 1161 grass species in panels **(a) – (i)**, **(p)**, **(q)** and **(u)** and 1729 in panels **(j) – (l)**, **(r)**, **(s)** and **(t)**.  
 1162 Corresponding regression coefficients for ahistorical analyses of relationships in panels **(a) – (l)**:  
 1163 0.14, 0.17, 0.14, 0.26, 0.34, 0.28, 0.24, 0.31, 0.26, 0.24, 0.29, and 0.3. Two-tailed  
 1164 phylogenetically reduced major axis (PRMA) regressions were fitted for  $\log(\text{trait}) = \log(a) + b$   
 1165  $\log(\text{trait})$  in panels **(a) – (l)** and **(p) – (u)**. Significance:  $***P < 0.001$ ,  $**P < 0.01$ .  $P =$  **(a)**  
 1166 0.0099, **(b)**  $7.8 \times 10^{-9}$ , **(c)**  $4.2 \times 10^{-9}$ , **(d)** 0.004, **(e)**  $1.8 \times 10^{-8}$ , **(f)**  $2.4 \times 10^{-11}$ , **(g)** 0.0014, **(h)**  $2.9 \times$   
 1167  $10^{-11}$ , **(i)**  $2.2 \times 10^{-13}$ , **(j)**  $1.7 \times 10^{-6}$ , **(k)**  $4.0 \times 10^{-7}$ , **(l)**  $1.1 \times 10^{-5}$ , **(p)**  $\sim 0$ , **(q)**  $\sim 0$ , **(r)**  $3.17 \times 10^{-219}$ ,  
 1168 **(s)**  $1.92 \times 10^{-205}$ , **(t)**  $7.92 \times 10^{-106}$  and **(u)**  $2.7 \times 10^{-96}$ .  $C_3$  and  $C_4$  species in red and blue,  
 1169 respectively.

1170

1171 **Extended Data Fig. 3. Worldwide association of grass leaf size with species' native climate**  
 1172 **in 3D, and binned by 1/3<sup>rd</sup> lowest, middle and highest mean annual temperature (MAT,**  
 1173 **°C), or mean annual precipitation (MAP, mm) in 2D. (a)** Leaf area ( $\text{cm}^2$ ) versus climate  
 1174 variables, i.e.  $x =$  mean annual temperature (MAT, °C) and  $y =$  mean annual precipitation (MAP,  
 1175 mm) in panel **(a)** and **(c)**, and the horizontal axes are flipped, i.e., leaf area versus  $x =$  MAP and  
 1176  $y =$  MAT in panels **(b)** and **(d)**. Relationships of **(e) – (g)** Leaf length, **(h) – (j)** leaf width, **(k) –**  
 1177 **(m)** leaf area, and **(n) – (p)** culm height with mean annual precipitation (mm);  $n = 584$  globally  
 1178 distributed grass species in panels **(e) – (m)** and 576 for panels **(n) – (p)**. Relationships of **(q) –**  
 1179 **(s)** Leaf length, **(t) – (v)** leaf width, **(w) – (y)** leaf area, and **(z) – (bb)** culm height with mean  
 1180 annual temperature (°C).  $N = 584$  globally distributed grass species in panels **(e) – (m)** and **(q) –**  
 1181 **(y)** and 576 for panels **(n) – (p)** and **(z) – (bb)**. Panels **(a)** and **(b)** present the data for all species  
 1182 in the global database ( $N = 1752$ ); panels **(c)** and **(d)** exclude the 29 species with  $\text{MAT} < 0$  °C,  
 1183 for a clearer view of the bulk of the species. Projected grey shadows in **(a) – (d)** represent the  
 1184 bivariate relationships. Parameters from multiple regression analysis are presented in  
 1185 Supplementary Table 8. Two-tailed ordinary least square (OLS) regressions were fitted for  $\log$   
 1186  $(\text{trait}) = \log(a) + b \log(\text{climate variable})$  in panels **(e) – (bb)**. Significance:  $***P < 0.001$ ,  $**P <$   
 1187  $0.01$ .  $P =$  **(e)**  $8.1 \times 10^{-5}$ , **(f)**  $2.2 \times 10^{-5}$ , **(g)** 0.0002, **(h)** 0.0094, **(i)**  $8.4 \times 10^{-28}$ , **(j)**  $1.7 \times 10^{-21}$ , **(k)**

1188 0.0002, **(l)**  $1.1 \times 10^{-20}$ , **(m)**  $1.8 \times 10^{-15}$ , **(n)** 0.0028, **(o)**  $4.7 \times 10^{-25}$ , **(p)**  $2.2 \times 10^{-10}$ , **(q)** 0.0106, **(r)**  
1189  $2.9 \times 10^{-6}$ , **(t)**  $7.0 \times 10^{-5}$ , **(u)**  $6.7 \times 10^{-6}$ , **(v)**  $1.5 \times 10^{-17}$ , **(w)** 0.0001, **(x)**  $7.9 \times 10^{-8}$ , **(y)**  $2.6 \times 10^{-11}$ ,  
1190 **(z)**  $1.3 \times 10^{-5}$ , **(aa)**  $1.7 \times 10^{-9}$  and **(bb)**  $8.5 \times 10^{-10}$ . C<sub>3</sub> and C<sub>4</sub> species in red and blue,  
1191 respectively.

1192

1193 **Extended Data Fig. 4. Quantile regression analyses of worldwide associations of grass leaf**  
1194 **traits with species' native climate.** Relationships of **(a) – (c)** Leaf length, **(d) – (f)** leaf width,  
1195 **(g) – (i)** leaf area, and **(j) – (l)** culm height with mean annual temperature (MAT, °C), mean  
1196 annual precipitation (MAP, mm) and aridity index (AI).  $N = 1752$  globally distributed grass  
1197 species in panels **(a) – (i)** and 1729 in panels **(j) – (l)**. Two-tailed ordinary least square (OLS;  
1198 solid lines) and 95% and 5% quantile regressions (dotted lines) were fitted for  $\log(\text{trait}) = \log$   
1199  $(a) + b \log(\text{climate variable})$ ; quantile lines drawn if significantly different in slope at  $P < 0.05$ .  
1200 C<sub>3</sub> and C<sub>4</sub> species in red and blue respectively.

1201

1202 **Extended Data Fig. 5. Worldwide associations of grass leaf and plant dimensions with**  
1203 **species' native climate, for species with leaf width < 8.16 cm or < 4.47 cm, i.e. below the**  
1204 **modelled threshold for damage due to night time chilling or overheating, and modeled leaf**  
1205 **temperature difference from air temperature for amphistomatous grass leaves under**  
1206 **different air temperatures.** Relationships of **(a) – (b)** Leaf length, **(c) – (d)** leaf width, **(e) – (f)**  
1207 leaf area, and **(g) – (h)** culm height with mean annual temperature (MAT, °C) and mean annual  
1208 precipitation (MAP, mm) for species with leaf width < 8.16 cm. Relationships of **(i) – (j)** Leaf  
1209 length, **(k) – (l)** leaf width, **(m) – (n)** leaf area, and **(o) – (p)** culm height with mean annual  
1210 temperature (MAT, °C) and mean annual precipitation (MAP, mm) for species with leaf width <  
1211 4.47 cm.  $N = 1748$  globally distributed grass species for panels **(a) – (f)**, 1725 for panels **(g) –**  
1212 **(h)**, 1716 for panels **(i) – (n)** and 1694 for panels **(o) – (p)**. Simulations were run with stomatal  
1213 conductance ( $\text{mol m}^{-2} \text{s}^{-1}$ ) **(q) – (t)** 0.1, **(u) – (x)** 0.2 and **(y) – (bb)** 0.4, and wind speed (m/s), at  
1214 **(q), (u) and (y)** 0.1, **(r), (v) and (z)** 0.5, **(s), (w) and (aa)** 1, **(t), (x) and (bb)** 2, with leaf width  
1215 (cm) of 0.04, 0.1, 0.5, 0.9, 1.5, 2.7 and 11 shown as increasing darker blue lines. No difference in  
1216 leaf temperature from air temperature line in red. Two-tailed ordinary least square (OLS)  
1217 regressions were fitted for  $\log(\text{trait}) = \log(a) + b \log(\text{climate variable})$  in panels **(a) – (p)**.  
1218 Significance: \*\*\* $P < 0.001$ , \*\* $P < 0.01$ , \* $P < 0.05$ .  $P =$  **(a)**  $2.1 \times 10^{-8}$ , **(b)**  $6.2 \times 10^{-13}$ , **(c)**  $4.7 \times$

1219  $10^{-29}$ , **(d)**  $6.2 \times 10^{-48}$ , **(e)**  $2.0 \times 10^{-24}$ , **(f)**  $6.8 \times 10^{-40}$ , **(g)**  $1.9 \times 10^{-24}$ , **(h)**  $1.3 \times 10^{-33}$ , **(i)**  $2.4 \times 10^{-7}$ ,  
1220 **(j)**  $7.4 \times 10^{-11}$ , **(k)**  $1.0 \times 10^{-26}$ , **(l)**  $3.4 \times 10^{-39}$ , **(m)**  $5.4 \times 10^{-22}$ , **(n)**  $9.8 \times 10^{-33}$ , **(o)**  $4.4 \times 10^{-22}$  and  
1221 **(p)**  $3.8 \times 10^{-29}$ . C<sub>3</sub> and C<sub>4</sub> species in red and blue respectively.

1222

1223 **Extended Data Fig. 6. Worldwide scaling of grass vein length per leaf area and vein**  
1224 **diameter with leaf size and species' native climatic aridity, and of vein xylem conduit**  
1225 **diameter with vein diameter.** Relationships of major vein length per area with **(a)** and **(c)** leaf  
1226 width, **(b)** and **(d)** leaf area and **(e)** aridity index (AI) (where lower values correspond to greater  
1227 climatic aridity). Relationships of vein diameters with **(f, i, l, o)** leaf length, **(g, j, m, p)** leaf  
1228 width and **(h, k, n, q)** leaf area (= leaf length  $\times$  leaf width). Relationships of vein length per area  
1229 with **(r, u, x, aa)** leaf length, **(s, v, y, bb)** leaf width and **(t, w, z, cc)** leaf area (leaf length  $\times$  leaf  
1230 width). Relationships of vein xylem conduit diameters with vein diameter **(dd)** first order (1°)  
1231 veins, **(ee)** second order (2°) veins, **(ff)** third order (3°) veins and **(gg)** fourth order (4°).  $N = 616$   
1232 species in panels **(a)**, 600 in panel **(b)**, 170 in panel **(c)**, 166 in panel **(d)**, 21 in panel **(e)**, 27 in  
1233 panels **(f) – (ff)** and 7 in panel **(gg)**. Two-tailed ordinary least square (OLS) regressions,  
1234 phylogenetic generalized least square (PGLS) or phylogenetic reduced major axis (PRMA)  
1235 regressions were fitted for  $\log(\text{trait}) = \log(a) + b \log(\text{trait or climate variable})$  in panels **(a)** and  
1236 **(b)**, **(c)** and **(d)**, and **(e)**, respectively. Phylogenetic reduced major axis (PRMA) or phylogenetic  
1237 generalized least square (PGLS) regressions were fitted for  $\log(\text{vein diameter or vein length per}$   
1238  $\text{area}) = \log(a) + b \log(\text{leaf length, width, or leaf area})$  in panels **(f) – (q)**, and **(r) – (cc)**,  
1239 respectively. Phylogenetic reduced major axis (PRMA) regressions were fitted for  $\log(\text{xylem}$   
1240  $\text{conduit diameter}) = \log(a) + b \log(\text{vein diameter})$  in panels **(dd) – (gg)**.  $P^* < 0.05$ ,  $P^{**} < 0.01$ ,  
1241  $P^{***} < 0.001$ .  $P =$  **(a)**  $9.4 \times 10^{-250}$ , **(b)**  $1.6 \times 10^{-139}$ , **(c)**  $7.0 \times 10^{-46}$ , **(d)**  $1.0 \times 10^{-31}$ , **(e)** 0.0051, **(f)**  
1242 0.0007, **(h)**  $3.0 \times 10^{-5}$ , **(i)**  $3.9 \times 10^{-6}$ , **(k)** 0.0003, **(s)**  $1.2 \times 10^{-34}$ , **(t)**  $7.0 \times 10^{-04}$ , **(v)**  $1.4 \times 10^{-7}$ , **(w)**  
1243 0.0167, **(bb)** 0.0020, **(dd)** 0.0110 and **(ee)** 0.0004. Line parameters for panels **(f) – (cc)** in Table  
1244 1 and Supplementary Table 10 and for **(dd) – (gg)** in Supplementary Table 11. Significant  
1245 relationships are plotted with PRMA to illustrate the central trends (see *Methods*). C<sub>3</sub> and C<sub>4</sub>  
1246 species in white and grey respectively. Standard errors for species trait values are found in  
1247 Supplementary Table 3.

1248

1249

1250 **Extended Data Fig. 7. Scaling of leaf vein projected area, vein surface area and vein volume**  
1251 **of given vein orders with leaf dimensions across 27 C<sub>3</sub> and C<sub>4</sub> grass species grown**  
1252 **experimentally.** Relationships of vein projected area with (a, d, g, j) leaf length, (b, e, h, k) leaf  
1253 width and (c, f, i, l) leaf area (leaf width × leaf length). Relationships of vein surface area with  
1254 (m, p, s, v) leaf length, (n, q, t, w) leaf width, and (o, r, u, x) leaf area (leaf length × leaf width).  
1255 Relationships of vein volume with (y, bb, ee, hh) leaf length, (z, cc, ff, ii) leaf width, and (aa, dd,  
1256 gg, jj) leaf area (leaf width × leaf length). Two-tailed phylogenetic generalized least square  
1257 (PGLS) regressions were fitted for log (vein projected area, vein surface area per area or vein  
1258 volume) = log (a) + b log (leaf length, width, or area) and drawn when significant.  $P^* < 0.05$ ,  
1259  $P^{**} < 0.01$ ,  $P^{***} < 0.001$ ; line parameters in Supplementary Table 10.  $P =$  (a) 0.0011, (b)  $1.2 \times$   
1260  $10^{-12}$ , (d) 0.0011, (e)  $7.0 \times 10^{-5}$ , (g) 0.0335, (h) 0.0161, (k) 0.0167, (m) 0.0011, (n)  $1.2 \times 10^{-12}$ ,  
1261 (p) 0.0011, (q)  $7.0 \times 10^{-5}$ , (s) 0.0335, (t) 0.0161, (w) 0.0167, (y)  $8.2 \times 10^{-6}$ , (z)  $5.4 \times 10^{-6}$ , (bb)  
1262  $5.2 \times 10^{-5}$ , (cc) 0.0037 and (ff) 0.0093. Significant trends are plotted with PRMA to illustrate the  
1263 central trends (see methods). Standard errors for species trait values are found in Supplementary  
1264 Table 3. C<sub>3</sub> and C<sub>4</sub> species in white and grey respectively.

1265

1266 **Extended Data Fig. 8. Partitioning of the contributions of given vein orders of the venation**  
1267 **architecture of C<sub>3</sub> and C<sub>4</sub> grasses, with minor veins accounting for the differences in vein**  
1268 **length per area.** (a) *Triticum aestivum*, a C<sub>3</sub> species. (b) *Aristida ternipes*, a C<sub>4</sub> species without  
1269 4° veins (C<sub>4-3L</sub>; i.e., third-order veins are the highest longitudinal vein order). (c) *Paspalum*  
1270 *dilatatum*, a C<sub>4</sub> species with 4° veins (C<sub>4-4L</sub>; i.e., fourth-order veins are the highest longitudinal vein  
1271 order). (d) Vein length per area (cm cm<sup>-2</sup>) distribution across vein orders for each type (C<sub>3</sub>  $n =$   
1272 11, C<sub>4-3L</sub> = 9, C<sub>4-4L</sub> = 7). (e) Vein length per unit area, (f) vein surface area per unit leaf area,  
1273 (g) vein projected area per unit leaf area and (h) vein volume per unit leaf area distribution  
1274 across vein orders for each type (C<sub>3</sub>  $n = 11$ , C<sub>4</sub> = 16). Statistical comparisons by phylogenetic  
1275 ANOVA are presented in Supplementary Table 3.

1276

1277 **Extended Data Fig. 9. Associations of light-saturated leaf photosynthetic rate with native**  
1278 **climate and vein traits for terrestrial C<sub>3</sub> species, and the scaling of transverse 5° vein length**  
1279 **per area (5° VLA) with major vein length per area (major VLA) across 27 C<sub>3</sub> and C<sub>4</sub> grass**  
1280 **species grown experimentally.** Relationships of area-based light-saturated photosynthetic rate

1281 ( $A_{\text{area}}$ ), measured with photosynthesis systems, with (a) mean annual temperature (MAT, °C), (b)  
1282 mean annual precipitation (MAP, mm), and (c) and growing season length (GSL, month).  
1283 Relationships of light-saturated photosynthetic rate per area with (d) major vein length per area  
1284 ( $VLA_{\text{major}}$ ,  $\text{cm cm}^{-2}$ ) and (e) major vein surface area per area ( $VSA_{\text{major}}$ , unitless), and (f)  
1285 (transverse vein length per area ( $VLA_{\text{transverse}}$ ,  $\text{cm cm}^{-2}$ ) with  $VLA_{\text{major}}$ . Points and lines in red  
1286 represent 8 terrestrial  $C_3$  grasses of this study grown in a greenhouse common garden, related to  
1287 the mean climate of their native distribution, supporting the assumption of higher photosynthetic  
1288 rate in colder and drier climates with shorter growing seasons. Open points represent 13  
1289 Northern Hemisphere temperate terrestrial  $C_3$  grass species from the global plant trait network  
1290 (GLOPNET; ref 126) measured in the field, as related to the mean climate at their field site.  
1291 Black lines represent the significant trend through all the points in panels (a) and (c), which,  
1292 given the disparate data sources combined here (and the consideration of field site rather than  
1293 native range climate for the GLOPNET species), provides yet stronger support for the generality  
1294 of the relationships of  $A_{\text{area}}$  to MAT and GSL. Notably, these are conservative tests of the  
1295 relationships of photosynthetic rate with native climate, as measurements of  $A_{\text{area}}$  using the  
1296 photosynthesis system chamber do not include the effect of the boundary layer conductance,  
1297 which is made very high and invariant<sup>23</sup>. Under natural conditions, and especially under slow  
1298 windspeeds, smaller leaves would have higher boundary layer conductances than larger leaves  
1299 (see simulation in Extended Data Fig. 5), and thus, under natural conditions, including the effects  
1300 of boundary layer, a yet stronger trend would be expected for small-leaved species of colder and  
1301 drier climates to have higher photosynthetic rates than larger-leaved species of warm, moist  
1302 climates. Two-tailed ordinary least square (OLS) regressions or phylogenetic reduced major axis  
1303 (PRMA) were fitted for  $\log(\text{trait}) = \log(a) + b \log(\text{trait or climate variable})$  in panels (a) – (e)  
1304 and (f), respectively. Significance:  $P^* < 0.05$ ,  $P^{**} < 0.01$ ,  $P^x = 0.04$  in a one-tailed test of the  
1305 hypothesized positive correlation.  $P =$  (a) 0.0301 red line; 0.0071 black line, (b) 0.0183, (c)  
1306 0.0474 red line; 0.0021 black line, (d) 0.0794, (e) 0.0138 and (f) 0.0061. Error bars represent  
1307 standard errors in panels (a) – (e). Standard errors for species trait values in panel (f) are found in  
1308 Supplementary Table 3.  $C_3$  and  $C_4$  species in white and grey, respectively, in panel (e).

1309

1310 **Extended Data Fig. 10. Estimating leaf size from venation traits that can be measured on**  
1311 **small samples or fragments of grass leaves. (a) Leaf area and (b) leaf width predicted from 2°**

1312 vein length per area.  $N = 600$  and  $616$  in panels **(a)** and **(b)** respectively (Grassbase dataset;  
1313 Supplementary Table 2). The relationships were fitted with two-tailed ordinary least square  
1314 (OLS) regressions. These relationships would enable the determination of intact leaf size from  
1315 fragments that include at least two  $2^\circ$  veins, including fragmentary fossil remains. The 95%  
1316 confidence intervals are in blue and 95% prediction intervals in red.  $P^{***} < 0.001$ .  $P = \mathbf{(a)} 1.4 \times$   
1317  $10^{-127}$  and  $\mathbf{(b)} 7.6 \times 10^{-227}$ .



